REPORT DOCUMENTATION PAGE

Form Approved OMB No. 0704-0188

1. AGENCY USE ONLY (Leave blank)	2. REPORT DATE	3. REPORT TYPE AND DATES COVERED
	13-April-2000	Final Report

4. TITLE AND SUBTITLE

CyMPA - Program For Analyzing Microstrip Patch Arrays On Circular-Cylindrical Structures

5. FUNDING NUMBERS

F61775-99-WE040

6. AUTHOR(S)

Assistant Professor Zvonimir Sipus

7. PERFORMING ORGANIZATION NAME(S) AND ADDRESS(ES)

University of Zagreb
Unska 3
Zagreb HR-10000
Croatia

8. PERFORMING ORGANIZATION REPORT NUMBER

N/A

9. SPONSORING/MONITORING AGENCY NAME(S) AND ADDRESS(ES)

EOARD
PSC 802 BOX 14
FPO 09499-0200

10. SPONSORING/MONITORING AGENCY REPORT NUMBER

SPC 99-4040

11. SUPPLEMENTARY NOTES

12a. DISTRIBUTION/AVAILABILITY STATEMENT

Approved for public release; distribution is unlimited.

12b. DISTRIBUTION CODE

A

13. ABSTRACT (Maximum 200 words)

This report results from a contract tasking University of Zagreb as follows: The contractor will investigate analyze arrays of rectangular patches on multilayer circular cylinder that is placed periodically in the circumferential and axial directions. The contractor shall investigate the following antenna characteristics: (a) current distribution at each patch in the array; (b) input impedance of each patch in the array; (c.) mutual coupling between each two patches in the array (d) radiation pattern of the array when all mutual couplings are taken into account; (e) radiation pattern of the array without taking mutual coupling into account (fast calculations of the radiation pattern needed for making the first design of the array).

14. SUBJECT TERMS

EOARD, Electromagnetics, Computational Electromagnetics, Antennas, Phased Arrays

15. NUMBER OF PAGES

48

16. PRICE CODE

N/A

17. SECURITY CLASSIFICATION OF REPORT	18. SECURITY CLASSIFICATION OF THIS PAGE	19, SECURITY CLASSIFICATION OF ABSTRACT	20. LIMITATION OF ABSTRACT
UNCLASSIFIED	UNCLASSIFIED	UNCLASSIFIED	UL

FINAL REPORT FOR CONTRACT **F61775-99-WE040**

CyMPA

Program for Analyzing Microstrip Patch Arrays on Circular-Cylindrical Structures

by

Zvonimir Sipus, PhD

SUBMITTED BY: Zvonimir Sipus
Faculty of Electrical Engineering and Computing
University of Zagreb
Unska 3
Zagreb, HR-10000, Croatia

13 April 2000

TABLE OF CONTENTS

1 INTRODUCTION

When constructing antennas it is popular to use printed metal patches on multilayer substrates to obtain thin profile, light weight and low manufacture cost. For their ability to conform the antenna structure (for example to conform the shape of a rocket or of an airplane), microstrip antennas are well suited to conformal antennas. Patch antennas and arrays on cylindrical structures offer a possibility either to cover 360 degrees in a plane perpendicular to the cylinder axis, or to create directed beams in arbitrary direction. The former possibility is important for missile applications, while the latter one is particularly useful in communications applications where there is a need for enlarging the capacity of the terminal antennas and for improving the quality of the signal.

Traditional approach of analyzing conformal antennas is to consider the antenna structure as a planar structure of infinite extent, which is a reasonable approximation if the radius of the structure curvature is large. However, when the radius of the curvature is small, we cannot neglect the curvature of the structure. For example, reducing the radius of the structure can significantly change the input impedance and the resonant frequency. We can obtain an omnidirectional radiation pattern with only one patch, which is impossible for planar patches. For such antennas more accurate analysis techniques should be used.

We have developed a program for analyzing microstrip patch arrays placed on circular cylinders, which rigorously takes into account the geometry of the antenna. The arrays are analyzed in the spectral domain, since the spectral approach shows a lot of advantages in analyzing cylindrical problems. The parameters of interest for calculation are radiation pattern, input port impedance, and mutual coupling between elements. Furthermore, the program is suitable for array synthesis, not only for analyzing already designed arrays. For that reason the program has less accurate fast part for making the first design of the array, and more accurate part (but computationally slower part) for making the final design.

2 PROBLEM IDENTIFICATION AND ITS SIGNIFICANCE

Conformal microstrip patch antennas have been proposed for a wide range of applications since they have potential advantages over planar antennas. Here, some of possible applications will be mentioned. They are mounted on smart missiles and rockets because they conform to the structure and therefore they do not disturb aerodynamic properties. Furthermore, it is possible to obtain the 360 degrees covering. Future military airborne and space based sensors will require active electronically scanned array antennas. Planar arrays are one solution. However, planar arrays can be electronically scanned to about 60 degrees from boresight, and the gain falls with scanning angle. The conformal arrays can scan the beam without drop of the gain, and the size of the conformal antenna needed for obtaining the same gain as in the planar case is approximately the same. For the same reason conformal arrays are a good candidate for future base station antennas where increased capacity of the network will be obtained by using multibeam narrow-beamwidth antennas. There is also a need for omnidirectional antennas for wireless applications, and a good candidate is a cylindrical patch antenna that is almost wrapped around. Finally, in commercial applications like cruise control for cars and distance monitoring for parking, a conformal antenna can be hidden to allow aesthetically looking product.

The traditional approach of analyzing conformal microstrip antennas is to approximate the conformal structure with locally planar one, and then to use some method form planar antennas. This is a reasonable approximation if the radius of the structure curvature is large. However, for small radiuses the properties of the antenna begin to be significantly different from their planar counterpart. Here we will mention what will change in the case of microstrip patch antennas printed on circular cylindrical structure. For axially polarized patch antennas the input impedance will significantly drop with reducing the structure radius. In benchmark four there is an example where the resonant resistance is 30% reduced by changing the structure radius from 0.67 wavelength to 0.17 wavelength. For patches polarized in circumferential direction the change of input impedance is opposite, i.e. input impedance will grow with reducing the structure radius. The amplitude of surface waves, and therefore mutual coupling, is enlarged in axial direction and reduced in circumferential direction (in comparison to the planar case). The radiation pattern can be drastically changed in circumferential direction. For example, we can get omnidirectional radiation pattern if the patch is almost wrapped-around, where in the planar case the backward radiation is always weak. The resonant frequency is almost the same for axially polarized patches, and it is significantly changed for patches polarized in circumferential direction.

When designing the conformal arrays there is a need to determine appropriate excitation distribution in order to achieve desirable radiation characteristics. The easiest approach is to use the projective synthesis, i.e. to project the known planar aperture distribution to conformal surface. However, this can give poor results. Better solution will be to use some optimization routine, like iterative least squares or genetic algorithm. In order to get good performances of the array and in order not to make the optimization process time consuming, there is a need for a program which analyze conformal arrays and which is computationally fast.

All this show the need for computer programs which will rigorously take into account the effects of the curvature, and which will help the engineers in designing the conformal antennas.

3 PROJECT OBJECTIVE AND REALIZED OUTCOMES

The goal of the project was to develop a program for analyzing the arrays of rectangular patches placed on multilayer circular cylinder. The assumed geometry of the array consists of rectangular patches which have the same dimensions, and which are placed periodically in the circumferential and axial directions. The number of dielectric layers can be arbitrary. However, it is very rarely in practice that more than three layers are used. Two types of feeding structure of each patch element are considered: coax feeding and microstrip line feeding. It was assumed that one patch can have several input ports.

It was planned that the program calculates the following antenna characteristics:

- current distribution at each patch in the array
- input impedance at each input port in the array
- mutual coupling between each two patches in the array
- radiation pattern of the array when all mutual couplings are taken into account
- radiation pattern of the array without taking mutual coupling into account (fast calculations of the radiation pattern needed for making the first design of the array).

We have developed two programs CyMPA and CyMPApat that calculate the parameters of the array. The reason for splitting the problem into two parts is that input impedance and mutual coupling is usually calculated for several frequency points which cover the frequency band of interest, and radiation pattern is usually calculated only at one frequency. For that reason program CyMPA calculates:

- current distribution at each patch in the array
- input impedance at each input port in the array
- mutual coupling between each two patches in the array

and program CyMPApat calculates

- radiation pattern of the array when all mutual couplings are taken into account
- radiation pattern of the array without taking mutual coupling into account

In order to determine the radiation pattern program CyMPApat is using the results of program CyMPA, i.e. the calculated current distribution is used. In the report we will name both programs CyMPA unless it is needed to distinguish between them.

Other tasks that are implemented in program CyMPA are:

- the considered cylindrical structure can be multilayer. From practical point of view the maximum number of layer is 10. However, this number can be easily enlarged if needed.

- two types of feeding structures can be analyzed: feeding by a coaxial transmission line and feeding by a microstrip transmission line. It is possible that each patch in the array is fed by several transmission lines, which is important to obtain the circular polarization. From practical point of view the maximum number of ports is 4. If needed, this number can be easily enlarged.

It was planned that the project outcome consists of two versions of the program for the analysis of patches fed by a microstrip line. Therefore, we have developed two models of this type of feeding structure: an approximate model which needs less computer time, and a complex model which rigorously takes into account the current distribution on the microstrip feeding line and in the region where the feeding line is attached to the patch. Paradoxically, the approximate model gave better results in all tried cases (and it needed much less computer time). Therefore we suggest using this version of the program for the antenna design and analysis.

The program is developed in FORTRAN since this program language is considered as the fastest language for computational applications. Program is independent on the machine, and it can be compiled and run on every machine that has FORTRAN 90 compiler. Furthermore, for PC environment, a graphical user interface is developed to make easy setting the input parameters, and to obtain graphical presentation of the results. On other machines communication with the program is made via input/output ASCII files. In other words, the input file should be filled before running the program, and the results are written into the output file that can be graphically presented by any graphical program. For case of simplicity, both CyMPA and CyMPApat programs have the same input file. Finally, it is possible to connect the program with the Touchstone program for analyzing microwave networks. This is done by producing the output file with S-parameters in a form defined by the authors of the Touchstone program.

4 PROJECT OUTCOMES

4.1 THEORETICAL BACKGROUND

4.1.1 MOMENT METHOD PROCEDURE

The geometry of the problem is shown in Figure 4.1. The rectangular patches are printed on circular-cylindrical substrate of radius ρ_{patch}. The substrate can be generally multilayered, and the radius of the cylindrical ground plane (tube) is ρ_{GND}. The dimensions of each patch are W_ϕ and W_Z , and the distances of the feeding point from the center of the patch in the ϕ and z directions are ϕ_{feed} and z_{feed}, respectively. Both microstrip line feeding and coax feeding are analyzed.

To determine the current on the patches, we consider the integral equation for electric field components tangential to the patches [1]:

$$\hat{\rho} \times (\mathbf{E}^{inc} + \mathbf{E}^{scat}) = 0 \qquad \text{on patches.} \tag{1}$$

By using the dyadic Greens function $\overline{\overline{\mathbf{G}}}$ for circular-cylindrical structure we get the following equation:

$$\begin{aligned} &\sum_n \iint_{patch} \overline{\overline{\mathbf{G}}}(\phi, z, \rho_{patch} \,|\, \phi', z', \rho_{patch}) \mathbf{J}^n_{patch}(\phi', z')\, dS \\ &+ \sum_n \iiint_{feed} \overline{\overline{\mathbf{G}}}(\phi, z, \rho_{patch} \,|\, \phi', z', \rho')\, \mathbf{J}^n_{feed}(\phi', z', \rho')\, dV' = 0 \quad \text{on patches.} \end{aligned} \tag{2}$$

Here $\mathbf{J}^n_{patch}$ and $\mathbf{J}^n_{feed}$ denote the current on the nth patch and on the nth feeding line, respectively. In the case of the coax feeding, the radius of the probe is usually a very small fraction of the wavelength and the quantity ρ_{patch} - ρ_{GND} is usually small in comparison to the wavelength. Therefore, the probe is modelled as a filament with a constant current

$$\mathbf{J}^n_{feed}(\phi', z', \rho') = \hat{\rho}\frac{1}{\rho'}\delta(\phi' - \phi^n_{feed})\,\delta(z' - z^n_{feed}) \qquad \rho_{GND} \le \rho' \le \rho_{patch}, \tag{3}$$

where ϕ^n_{feed} and z^n_{feed} are the ϕ and z coordinates of the coax probe of the nth patch. The microstrip line can be also simply modelled by a filament with a constant current placed close to the edge of the patch since microstrip line and coax line have simillar field distribution around the feeding point. Furthermore, if the feeding point of the coax line is close to the patch edge, the input impedances of the patch antennas fed by a microstrip line and fed by a coax line are very simillar [2] - [4].

The unknown patch current is expanded into sum of the basis functions:

$$\mathbf{J}_{patch}(\phi, z) = \sum_i \alpha_i \mathbf{J}_i(\phi, z). \tag{4}$$

The unknown coefficients α_i are determined by applying the moment method (MoM). We have used the same test functions as basis functions (Galerkin's method). The elements of the impedance matrix [Z] and voltage vector [V] inside the moment method are calculated in the spectral domain. We use the one-dimensional Fourier transformation in the z direction and the Fourier series in the φ direction, defined by

$$\tilde{f}(m, k_Z, \rho) = \int_{-\infty}^{\infty}\int_{-\pi}^{\pi} f(\phi, z, \rho)\, e^{jm\phi} e^{jkzZ}\, d\phi\, dz. \tag{5a}$$

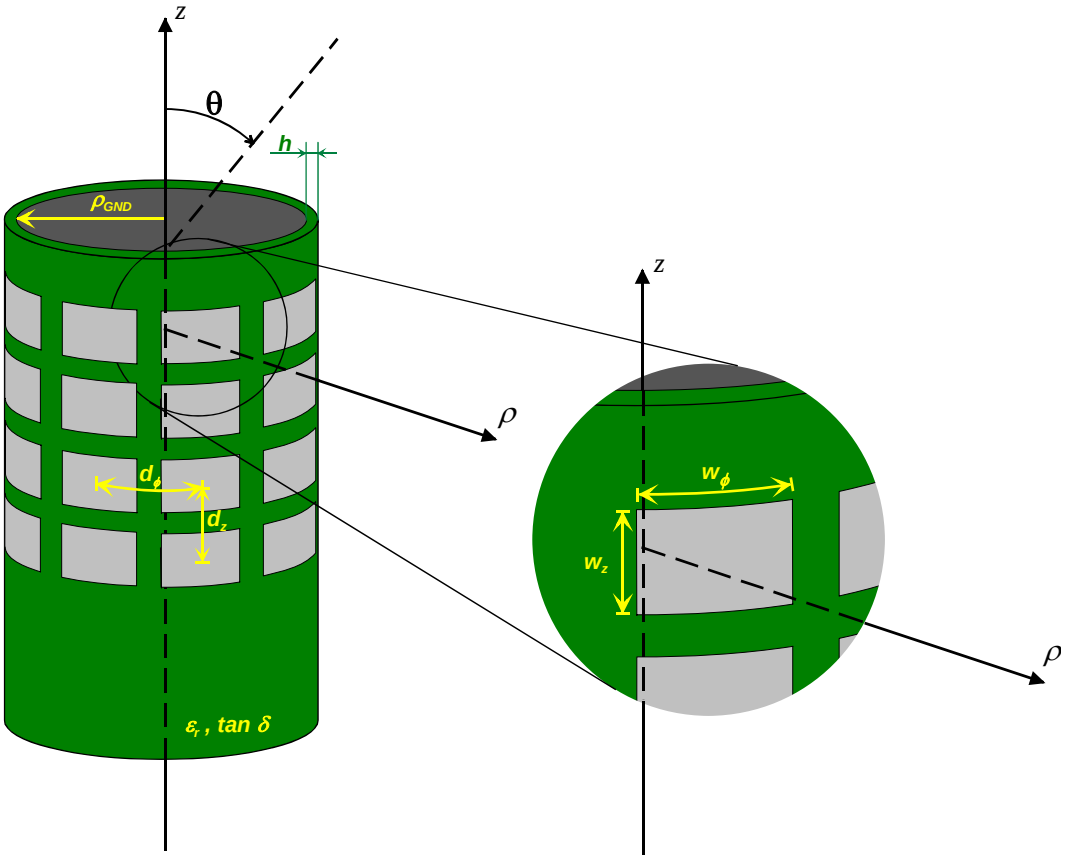

Fig. 4.1 - The geometry of the cylindrical patch array

$$f(\phi,z,\rho)=\frac{1}{4\pi^2}\sum_{-\infty}^{\infty}\int_{-\infty}^{\infty}\tilde{f}(m,k_Z,\rho)\;e^{-jm\phi}e^{-jkzZ}dk_Z. \tag{5b}$$

The elements of the impedance matrix [Z] and voltage vector [V] can be expressed as:

$$Z_{ij}=\frac{1}{4\pi^2}\sum_{-\infty}^{\infty}\int_{-\infty}^{\infty}\tilde{\mathbf{J}}_i(-m,-k_Z)\,\overline{\overline{\tilde{\mathbf{G}}}}(m,k_Z,\rho_{patch}|\rho_{patch})\,\tilde{\mathbf{J}}_j(m,k_Z)\,dk_Z$$

$$V_i=\frac{1}{4\pi^2}\sum_{-\infty}^{\infty}\int_{-\infty}^{\infty}\int_{feed}\tilde{\mathbf{J}}_i(-m,-k_Z)\,\overline{\overline{\tilde{\mathbf{G}}}}(m,k_Z,\rho_{patch}|\rho')\,\hat{\rho}e^{jkzZ^n_{feed}}\;e^{jm\phi^n_{feed}}\;d\rho'dk_Z\;. \tag{6}$$

4.1.2 Green's function calculation

The Green's functions are determined in spectral domain, which was one of the reasons to use spectral approach. For single layer structure we have used analytic expressions (see [1]), and for multilayer structure we have used the G1DMULT algorithm for numerical calculation of Green's functions for structures with arbitrary number of layers. The analytic approach needs less computer time than numerical approach. However, the analytic approach requires the complete derivation of Green's functions for each different structure, i.e., for any different number of layers.

The algorithm G1DMULT calculates spectral-domain Green's functions of circular cylindrical, planar and spherical multilayer structures (see [5] for details). The algorithm for the cylindrical case is illustrated in Fig. 4.2. The original 3D problem (Fig. 4.2.a) is transformed to the spectral domain (Fig. 4.2.b) by performing the Fourier transformation defined by eq. (5). The sources in the spectral domain are interpreted in space as a spectrum of current tubes of the form $e^{-jm\phi}e^{-jk_zz}$. Since the patches are infinitely thin in ρ-direction and since they have the same radius, for each m and k_z we get one current tube as a Fourier transformation of the array current. Each current tube excites cylindrical waves, one propagating away from the current tube and a standing cylindrical wave inside the tube (the expressions for E- and H-fields excited by current tube are given in [1]). The presence of the multilayer structure will cause a number of transmitted and reflected waves in each layer, with variation $e^{-jm\phi}$ and e^{-jk_zz} in the ϕ- and z-directions. Notice that all the waves have the same field variation in the ϕ- and z-directions for all layers, which is a consequence of the boundary conditions. Therefore, the problem of determining the Green's functions is a harmonic 1D problem in space with known harmonic variation in ϕ- and z-directions and unknown variation in ρ direction. We have to solve this 1D problem for a spectrum of m and k_z, and in order to find the 3D solution we must combine the solutions by a summation over the complete m and k_z spectrum, corresponding to an inverse Fourier transformation.

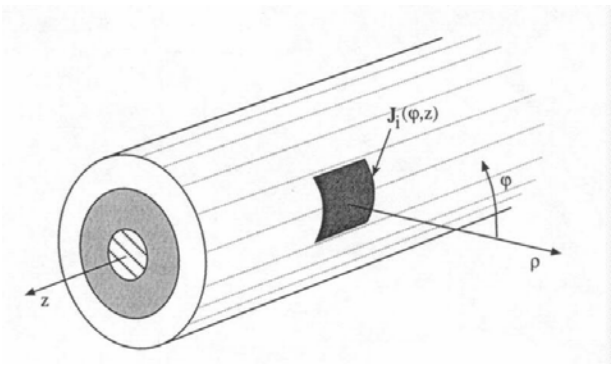

(a) 3-D Problem

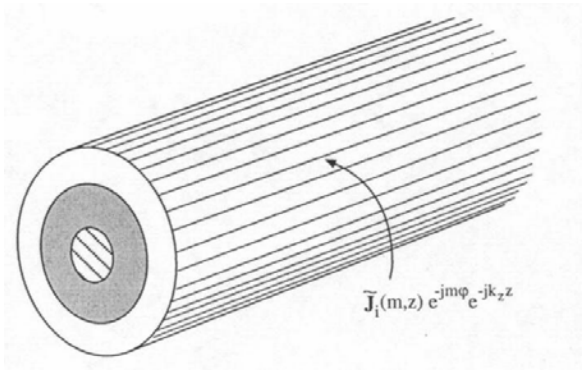

(b) Harmonic 1-D Problem

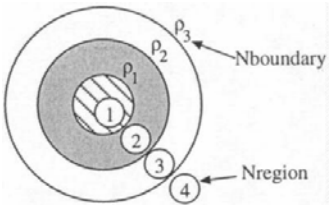

(c) Definition of material boundaries and regions (Nnregion extends to infinity)

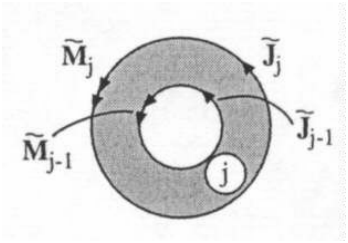

(d) Equivalent problem of region j
Equivalent currents are:

$$\tilde{\mathbf{J}} = \mathbf{n} \times \tilde{\mathbf{H}}_{\text{boundary}}$$

$$\tilde{\mathbf{J}} = -\mathbf{n} \times \tilde{\mathbf{E}}_{\text{boundary}}$$

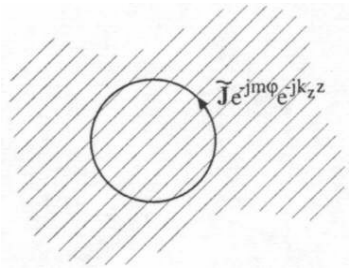

(e) The basic homogeneous harmonic 1-D field problem

Fig. 4.2 - Structuring of a 3D field problem with a circular cylindrical layered structure into a harmonic 1D problem and its subproblems. The G1DMULT subroutine solves the harmonic 1D problem.

The algorithm G1DMULT is based on subdividing the spatial harmonic problem into one equivalent problem per layer (Figs. 4.2.c and d), where the field in each region is formulated as the field radiated by equivalent currents at the layer boundaries. For example, the E-field in the layer *j* is expressed as

$$\tilde{\mathbf{E}}_j = \tilde{\mathbf{G}}^{\text{hom}}_{EJ} \tilde{\mathbf{J}}_{j-1} + \tilde{\mathbf{G}}^{\text{hom}}_{EJ} \tilde{\mathbf{J}}_j + \tilde{\mathbf{G}}^{\text{hom}}_{EM} \tilde{\mathbf{M}}_{j-1} + \tilde{\mathbf{G}}^{\text{hom}}_{EM} \tilde{\mathbf{M}}_j + \tilde{\mathbf{G}}^{\text{hom}}_{EJ} \tilde{\mathbf{J}}^{exci}_j + \tilde{\mathbf{G}}^{\text{hom}}_{EM} \tilde{\mathbf{M}}^{exci}_j \qquad (7)$$

where $\tilde{\mathbf{J}}_j$ and $\tilde{\mathbf{M}}_j$ are equivalent electric and magnetic current sheets at boundary *j*, $\tilde{\mathbf{J}}^{exci}_j$ and $\tilde{\mathbf{M}}^{exci}_j$ are excitation electric and magnetic currents in layer *j* (if any), and $\tilde{\mathbf{G}}^{\text{hom}}$ is the Green's function of the homogeneous problem (see [1]). By using $\tilde{\mathbf{J}}_j = \pm \hat{z} \times \tilde{\mathbf{H}}_j$ and $\tilde{\mathbf{M}}_j = \mp \hat{z} \times \tilde{\mathbf{E}}_j$ eq. (7) can be expressed in terms of the unknown tangential E- and H-fields $\tilde{\mathbf{E}}_j$ and $\tilde{\mathbf{H}}_j$ at the boundary *j* between layers *j* and *j+1* and known excitation currents. The boundary conditions that the tangential E- and H-fields are continuous at the layer boundaries give 4 linear equations per boundary. The tangential E- and H-fields are evaluated by solving the system of $4(N_{layer}-1)$ equations with $4(N_{layer}-1)$ unknowns, where N_{layer} is the number of layers in the multilayer structure. After they have been determined, the total E- and H-fields at any desired ρ-location can be found by using the equivalent problem in Fig. 4.2.d.

The core of G1DMULT is two subroutines G1DJ and G1DM for calculation of the fields radiated by electric and magnetic current sheets in an infinite homogeneous material (Fig. 4.2.e). The rest of the Fortran G1DMULT routine is simply a programming of the logical layout of the algorithm. More details about the G1DMULT algorithm can be found in [5].

4.1.3 Selection of basis function

As basis functions we have used the entire-domain basis functions, i.e., the basis functions which are defined on the whole patch. They are sinusoidal in the current direction and they are of constant/sinusoidal distribution in the perpendicular direction, which is a common approximation since patch antennas are resonant structures. We have divided the basis functions into three sets (the criteria was to which irreducible representation of the C_{2v} point group the particular basis function belongs, see Appendix for details). If the x-axis is going through the center of the patch and if the z-axis is the axis of the cylinder, then these three sets are (Fig. 4.3):

(A1) functions that are invariant under the reflection through the xy and xz planes:

$$\mathbf{J}_{kl}(\phi, z) = \hat{\phi}\, f(2k, 2l) + \hat{z}\, g(2k, 2l), \tag{8a}$$

(B1) functions that are invariant under the reflection through the xy plane and change sign under reflection through the xz plane:

$$\mathbf{J}_{kl}(\phi, z) = \hat{\phi}\, f(2k+1, 2l) + \hat{z}\, g(2k+1, 2l), \tag{8b}$$

(B2) functions that are invariant under the reflection through the xz plane and change sign under reflection through the xy plane:

$$\mathbf{J}_{kl}(\phi, z) = \hat{\phi}\, f(2k, 2l+1) + \hat{z}\, g(2k, 2l+1). \tag{8c}$$

Here k,l = 0,1, ... , and functions f and g are defined by

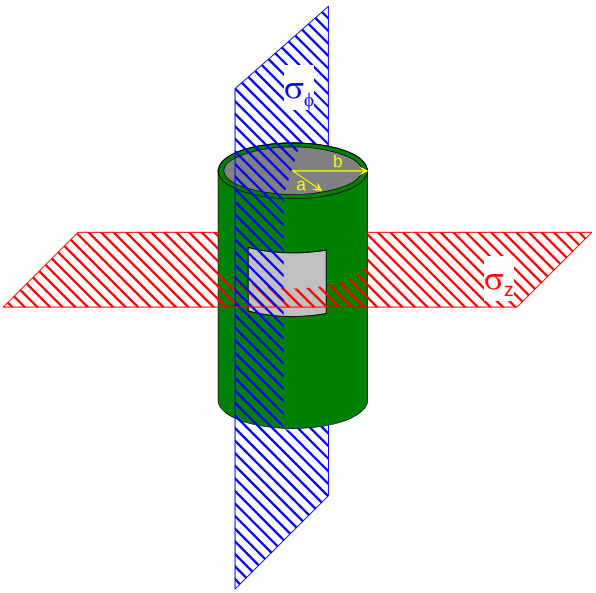

Fig. 4.3 - The symmetry operations of a rectangular patch antenna printed on a circular cylindrical structure.

$$f(k,l) = \left(\frac{k\pi}{W_\phi}\right)\sin\left(\frac{k\pi}{W_\phi}(\phi + W_\phi/2)\right)\cos\left(\frac{l\pi}{W_Z}(z + W_Z/2)\right)$$
$$g(k,l) = \left(\frac{l\pi}{W_Z}\right)\cos\left(\frac{k\pi}{W_\phi}(\phi + W_\phi/2)\right)\sin\left(\frac{l\pi}{W_Z}(z + W_Z/2)\right). \quad (9)$$

The fourth set of basis functions, i.e., the basis functions which change sign under reflections through both planes, we did not use. The advantage of this division of basis functions is that the Z_{ij} elements of basis and test functions defined at the same patch and belonging to different sets are zero. Furthermore, if the basis and test functions are belonging to different patches, then the term $e^{jm\Delta_\phi}\, e^{jkz\Delta_Z}$, appearing in the Fourier transformation of basis and test functions, is reduced to sinus/cosine functions as shown in Table 4.1 (Δ_ϕ and Δ_z are the distances between the centers of basis and test function in ϕ and z direction, respectively). This changing of exponential function is needed if we want to reduce the borders of integration and summation in the inverse Fourier transformation from (-∞, ∞) to (0, ∞).

	(A1)	(B1)	(B2)
(A1)	cos $m\Delta_\phi$ cos $k_z\Delta_z$	j cos $m\Delta_\phi$ sin $k_z\Delta_z$	j sin $m\Delta_\phi$ cos $k_z\Delta_z$
(B1)	j cos $m\Delta_\phi$ sin $k_z\Delta_z$	cos $m\Delta_\phi$ cos $k_z\Delta_z$	- sin $m\Delta_\phi$ sin $k_z\Delta_z$
(B2)	j sin $m\Delta_\phi$ cos $k_z\Delta_z$	- sin $m\Delta_\phi$ sin $k_z\Delta_z$	cos $m\Delta_\phi$ cos $k_z\Delta_z$

Table 4.1. Reduction of exponential function $e^{jm\Delta_\phi}\, e^{jkz\Delta_Z}$ appearing in the inverse Fourier transformation.

4.1.4 Numerical considerations

The expressions for the electromagnetic field due to the current tube contain Bessel and Hankel functions [5]. To improve the numerical efficiency we tabulate their values for the arguments needed in the G1DMULT routine, i.e., for each k_z we make a table of the values of the Bessel and Hankel functions for all m and for all arguments $\sqrt{k_n^2 - k_z^2}\,\rho$ corresponding to the ρ-coordinates of the boundaries and of the source and observation points. The reason for doing this is that an mth order Bessel/Hankel function in most commercial libraries is calculated in the recursive way by evaluating all Bessel/Hankel functions from 0th to mth order, which is not very time efficient unless storing and reusing intermediate results like we do.

We notice numerical problems in calculating Bessel/Hankel functions of large order (e.g. of order larger than 200; this happens when the radius of the structure is large). Therefore, for large-order Bessel and Hankel functions we use Debye's asymptotic formulas [6]:

$$J_m(x) \cong \frac{e^{m(\alpha - \tanh\alpha)}}{\sqrt{2\pi\tanh\alpha}}\left[1 + \frac{3t - 5t^3}{24m}\right] \quad (10a)$$

$$Y_m(x) \cong \frac{e^{m(\tanh\alpha - \alpha)}}{\sqrt{0.5\pi\tanh\alpha}}\left[1 - \frac{3t - 5t^3}{24m}\right]. \quad (10b)$$

Here Y_m is the Neumann function of order m ($H_m^{(2)} = J_m - jY_m$), $\cosh\alpha = m/x$, and $t = \coth\alpha$. Notice that the exponential parts of Bessel and Neumann approximate formulas have opposite behavior, i.e. the arguments of the exponential functions have the same absolute values and opposite signs. On the other hand Green's functions for cylindrical multilayer structures can be written in terms of products

$J_m(\cdot)H_m^{(2)}(\cdot)$ (see [5] for exact expressions). Therefore, Debye's asymptotic formulas are applied to products $J_m(\cdot)H_m^{(2)}(\cdot)$ with extracted exponential parts, and thereby, we avoid numerical problems.

Spectral-domain Green's functions contain poles that correspond to the propagation constants of surface wave modes [7]. For dielectrics without losses these poles are located on k_z axis between k_0 and k_n^{MAX}, where k_0 is the wave number in free-space and k_n^{MAX} is the maximum possible wave number, i.e. wave number of the region with maximum permittivity. If there are losses in the dielectric structure, the poles are located below the k_z axis. In order to avoid the difficulties with the integration around the poles of the Green's function, the contour of integration is moved from the poles (the Green's functions are analytical functions). The used contour is shown in Fig. 4.4.

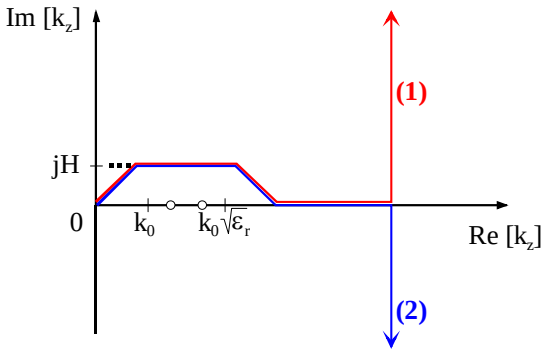

Fig. 4.4 - Path of integration in complex k_Z plane.

Furthermore, in order to make the inverse Fourier transformation more efficient in terms of computer time, the Fourier transforms of basis and test functions are written as a sum of exponential functions. For example, the Fourier transformation of the basic mode (basis function) in z-direction is written as

$$\tilde{g}^{(0,1)}(m,k_z) = \left(\frac{\pi}{W_z}\right)^2 \frac{e^{jk_zW_z/2} + e^{-jk_zW_z/2}}{(\pi/W_z)^2 - k_z^2} \tag{11}$$

For each term of the product of the basis and test function the path of the integration is selected in the way that the considered term decreases exponentially [8], see Fig. 4.3. In other words, the terms of the type $e^{j\xi k_z}$ are using the path (1) in Fig. 4.3, and the terms of the type $e^{-j\xi k_z}$ are using path (2).

We have tried the to model patch antennas fed by microstrip line in a rigorous way [9]. The currents on the feed line was modelled as a quasi-transverse electromagnetic (TEM) traveling wave current. Special care was taken to model the current at region where the microstrip line attach the patch. However, the calculated input impedance was too big for several test cases. This problem was also noticed in [10], where similar program was developed. Furthermore, the rigorous approach needs much more computer time. Therefore, the simple feed model have been implemented in the CyMPA program since the simple approach gives better results (in comparison with measurements), and it needs less computer time.

4.1.5 Array analysis

If we have N patches in the array, then we have to solve the linear system $[Z][\alpha^n] = [V^n]$ N times (n = 1,...,N), for each excitation port. In more details, $[V^n]$ vectors correspond to a physical situation in which a unit current is entering the nth port while the remaining N-1 ports are open-circuited. Fortunately, the

matrix [Z] is unchanged in all cases. After determining the amplitudes of basis functions [α^n] we calculate the voltage at port m by summation $-\sum_i V_i^m \alpha_i^n$, i.e., the mn element of the impedance port matrix is

$$Z_{mn}^{port} = -\sum_i V_i^m \alpha_i^n \ . \tag{12}$$

Scattering matrix elements are calculated from the impedance port matrix:

$$[S] = ([Z^{port}] - [Z^0])\,([Z^{port}] + [Z^0])^{-1} \tag{13}$$

where [Z^0] is a diagonal matrix with elements Z^0, the characteristic impedance of the feeding transmission lines.

If each port of the array is connected to a current source I_n^{port}, $n = 1,\ldots,N$, then the amplitudes of basis functions are calculated by

$$\alpha_i = \sum_{n=1}^{N} \alpha_i^n I_n^{port} \ . \tag{14}$$

If each port is connected to a voltage generator U^n with the internal impedance Z_n^L, the current amplitudes at each port are calculated by

$$[I^{port}] = ([Z^{port}] + [Z^L])^{-1}[U]. \tag{15}$$

After determining the port currents the amplitudes of basis functions are determined like for the current sources.

4.1.6 Far-field calculations

The far field is calculated as follows. If we consider the z component of the electric field in spectral domain, then only the outward travelling waves are propagating which are described with the Hankel function of the second kind $H_m^{(2)}$. Therefore, in the outermost region we can connect the z component of the electric field with different ρ components as

$$\tilde{E}_Z(m,k_Z,\rho_1) = \tilde{E}_Z(m,k_Z,\rho_2)\frac{H_m^{(2)}(k_\rho\rho_1)}{H_m^{(2)}(k_\rho\rho_2)}. \tag{16}$$

Similar equation is valied for $\tilde{H}_Z$. By choosing the component ρ_1 as the far field radius and ρ_2 as the ρ-component of the tube in the outermost region which has ρ larger than ρ-component of the patches ρ_{patch}, we get the values of the far field in spectral domain. $\tilde{E}_Z(m,k_Z,\rho_2)$ is equal to

$$\tilde{E}_Z(m,k_Z,\rho_2) = \sum_n \hat{z}\,\overline{\overline{\tilde{\mathbf{G}}}}(m,k_Z,\rho_2|\rho_{patch})\,\tilde{\mathbf{J}}_{patch}^n(m,k_Z). \tag{17}$$

The k_Z integral (eq. (5b)) can be computed approximately for large ρ by using saddle point method [11]

$$\frac{1}{2\pi}\int_{-\infty}^{\infty} f(k_Z)\,H_m^{(2)}(k_\rho\rho)\,e^{-jk_Z z}\,dk_Z \cong j^{(m+1)}\,\frac{1}{\pi}\,f(k_0\cos\theta)\,\frac{e^{-jk_0 r}}{r} \tag{18}$$

where r, θ, and ϕ are coordinates in the spherical coordinate system Thereby, in performing the inverse Fourier transformation we use only one k_Z value, $k_Z = k_0 \cos\theta$, and the remain sumation (inverse Fourier series) is made in the program. For the maximum value in the sumation over m in far-field calculations we use the value $N_{max} = 2\,k_0\,\rho_{patch}$.

The θ and ϕ componets of the electric far-field can be expressed as:

$$\begin{aligned} E_\theta^{FAR} &\cong -\frac{E_Z^{FAR}}{\sin\theta} & H_\theta^{FAR} &\cong -\frac{H_Z^{FAR}}{\sin\theta} \\ E_\phi^{FAR} &\cong -\eta_0 H_\theta^{FAR} & E_\phi^{FAR} &\cong \frac{1}{\eta_0} E_\theta^{FAR} \end{aligned} \tag{19}$$

Here η_0 is the impedance of free-space. By combining eqs. (16)-(19) we get the expressions for the far field. If we want to analyse the antenna for circular polarization, the right-hand and left-hand circular polarization component are determined by following expressions

$$E_{RHCP}^{FAR} = \frac{1}{\sqrt{2}}\,(E_\theta^{FAR} - jE_\phi^{FAR}) \qquad E_{LHCP}^{FAR} = \frac{1}{\sqrt{2}}\,(E_\theta^{FAR} + jE_\phi^{FAR}). \tag{20}$$

4.1.7 Appendix

We have applied the Galerkin's moment method procedure to calculate the performances of cylindrical microstrip antennas. There are two main classes of basis functions for the moment method procedure, the entire-domain and the sub-domain basis functions. When the latter are used, the procedure is more general but a larger number of basis functions has to be taken into account. The entire domain functions are more suitable for a simpler procedure, specially if we want to analyze microstrip arrays by using the element-by-element approach .

The calculations of the impedance matrix elements consume most of the computer time. Suitable choice of the entire domain basis functions puts many *Zij* elements of the impedance matrix equal to zero [12]. For simple cases odd or even property of basis functions provides the information which of the *Zij* elements are equal to zero. Same level of simplicity cannot be applied for complicated basis functions.

An alternative way for selecting suitable basis functions and determining the *Zij* elements equal to zero is to use symmetries that are present on the antenna. The patch shape generally possesses some symmetry, i.e. the shape is invariant under some reflections and/or rotations. Let **E** be an electric field caused by a current **J** with domain on the patch, and let L denote an operator which assigns **E** to **J**, **E** = L(**J**). It can be shown that L is invariant under the symmetry operations present on the patch on condition that the grounded dielectric slab fulfills the same symmetry operations (similarly as in [13]). Therefore, the following results of the group representation theory can be applied.

Definition [14]. A function $\mathbf{J}^{(\alpha,k)}(\phi, z)$ is said to belong to the kth row of the irreducible representation $\{D^\alpha(R)\}$ if

$$\frac{n_\alpha}{h}\sum_R D^\alpha(R)^*_{kk}\cdot O_R(\mathbf{J}^{(\alpha,k)}(\phi,z)) = \mathbf{J}^{(\alpha,k)}(\phi,z)\,, \tag{21}$$

where $D^{\alpha}_{kk}(R)$ denotes the *kk* element of the matrix $D^{\alpha}(R)$, *R* is the group element, O_R is the symmetry operator, *h* is the number of group elements, n_α is the dimensionality of the irreducible representation and asterisk (*) is complex conjugate.

Theorem [15]. Matrix elements of an operator *L* which is invariant under all operations of a group, vanish between functions belonging to different irreducible representations or to different rows of the same unitary representation.

Consequently, the Z_{ij} elements of the impedance matrix are given by

$$Z_{i(m,\alpha,k)\ j(n,\beta,l)} = <\tilde{\mathbf{J}}_m^{(\alpha,k)}, L(\tilde{\mathbf{J}}_n^{(\beta,l)})> = const \cdot \delta_{\alpha,\beta}\ \delta_{k,l}\ , \tag{22}$$

where $\tilde{\mathbf{J}}_m^{\alpha,k}$ denotes the *m*th basis function of the *k*th row of the irreducible representation $D^{\alpha}(R)$, $\delta_{k,l}$ is Kronecker's symbol and $<\cdot,\cdot>$ is the scalar product. The impedance matrix has a block diagonal form. The blocks are built using functions that belong to the same row of the same unitary irreducible representation. Furthermore, if the feed also possesses some of the patch symmetry properties, several terms of the voltage vector are equal to zero. The basis functions belonging to those irreducible representations will have coefficients equal to zero and therefore they can be excluded from calculations.

Example - rectangular patch antenna on circular cylindrical structure. The point symmetry group of the rectangular patch on circular cylindrical structure is C_{2v}. If the *x*-axis is going through the center of the patch and if the *z*-axis is the axis of the cylinder, then the symmetry operations that generate the group are reflections through the *xz* and *xy* planes (Fig. 4.3). There are four one-dimensional irreducible representations of C_{2v} denoted by A_1, A_2, B_1 and B_2. Their forms are given in Table 1. A draft of functions belonging to different representations is shown in Fig. 4.5. (Note that the unit vector that is perpendicular to the reflection plane changes the orientation under reflection.) If the basis functions are derived from the eigenmodes of the usual magnetic wall cavity model of the planar rectangular patch, they can be sorted using this draft:

(A1) functions that are invariant under the reflection through the *xy* and *xz* planes (Fig. 4.5.a):

$$\mathbf{J}_{kl}(\phi,z) = \hat{\phi}\, f(2k,2l) + \hat{z}\, g(2k,2l), \tag{23a}$$

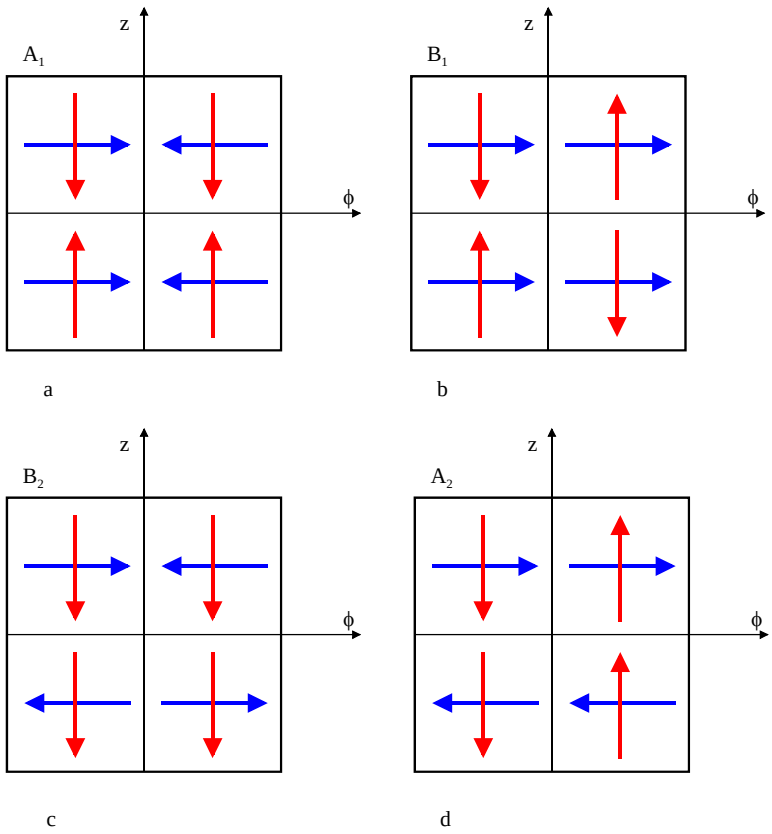

Fig. 4.5 - Draft of functions belonging to different irreducible repreentations of the point group C_{2v}.

(B1) functions that are invariant under the reflection through the *xy* plane and change sign under reflection through the *xz* plane (Fig. 4.5.b):

$$\mathbf{J}_{kl}(\phi,z) = \hat{\phi}\, f(2k+1,2l) + \hat{z}\, g(2k+1,2l), \tag{23b}$$

(B2) functions that are invariant under the reflection through the *xz* plane and change sign under reflection through the *xy* plane (Fig. 4.5.c):

$$\mathbf{J}_{kl}(\phi,z) = \hat{\phi}\, f(2k,2l+1) + \hat{z}\, g(2k,2l+1). \tag{23c}$$

(A2) functions that change sign under both reflections (Fig. 4.5.d):

$$\mathbf{J}_{kl}(\phi,z) = \hat{\phi}\, f(2k+1,2l+1) + \hat{z}\, g(2k+1,2l+1). \tag{23d}$$

Here $k,l = 0,1, \ldots$, and functions f and g are defined by eq. (9).

	E	σ_z	σ_ϕ	$\sigma_z \circ \sigma_\phi$
A_1	[1]	[1]	[1]	[1]
A_2	[1]	[-1]	[-1]	[1]
B_1	[1]	[1]	[-1]	[-1]
B_2	[1]	[-1]	[1]	[-1]

Table 4.2 - Irreducible representations of the point group C_{2v}. E is identity, σ_z and σ_ϕ are reflections though xy and xz planes.

Other selections of basis functions belonging to different irreducible representations are possible. Following the stated theorem, the Z_{ij} elements of the impedance matrix are equal to zero for the products of the functions belonging to different rows of term (23). If we further put the feed on the ϕ or z axis, then the voltage terms become equal to zero for two types of the basis functions and those basis functions can be omitted.

4.2 CyMPA - USER'S MANUAL

4.2.1 INTRODUCTION TO CyMPA

This chapter gives the user's manual for the program CyMPA. Since there are different requirements on calculation of radiation pattern and input impedance/mutual coupling, we have actually developed two programs CyMPA and CyMPApat. The main reason for splitting the problem into two parts is that radiation pattern is usually calculated only for one frequency, while input impedance and mutual coupling is usually calculated for frequency band of interest (and therefore even hundreds of frequency points can be calculated). Therefore, program CyMPA calculates

- current distribution at each patch in the array
- input impedance at each input port in the array
- mutual coupling between each two patches in the array,

and program CyMPApat calculates

- radiation pattern of the array when all mutual couplings are taken into account
- radiation pattern of the array without taking mutual coupling into account

In order to determine the radiation pattern, program CyMPApat is using the results of program CyMPA, i.e. current distribution calculated at selected frequency point is used.

Program is written in FORTRAN 90, and therefore can be compiled and run at each machine where FORTRAN 90 is installed or which support the executable version of the program. The communication with the program is made via input/output ASCII files. For case of simplicity, both programs CyMPA and CyMPApat are using the same input file (cympa.in). The detailed description of input and output files are given in this chapter.

We have also developed a graphical user interface is for PC computers. By this it is easier to define the input parameters, and to obtain graphical presentation of the results. Programs CyMPA and CyMPApat are working independently of graphical user interface, i.e., graphical user interface is used only for writing the input file, running the CyMPA and CyMPApat programs, reading the output files, and displaying the results. The description of graphical user interface is also given in this chapter.

4.2.2 PROBLEM DOMAIN DESCRIPTION

The CyMPA and CyMPApat programs analyze microstrip patch antennas or antenna arrays placed on cylinders, as illustrated in fig. 4.6. If an array is analyzed, following assumptions are made:

- all antenna elements are identical, both in terms of dimensions and feed/port types
- the patch elements are of rectangular shape (with equal or unequal sides)
- constant spacing between neighboring patches in circumferential (ϕ) direction
- constant spacing between neighboring patches in axial (z) direction
- the dielectric structure can be multilayered with losses
- the patch array must be placed at the top of one such layer
- either coax or microstrip line feeding ports can be analyzed
- multiple ports can be defined on patch, e.g. when designing circularly polarized arrays

By means of CyMPA program current distribution at each patch in the array can be calculated, as well as input impedance at each input port, and mutual coupling between each two patches.

The CyMPApat program calculates then radiation pattern of the array, with taking mutual coupling into account. If a first / fast design of an array is performed, CyMPApat can be applied as a standalone program, which gives less accurate, but fast radiation pattern information data.

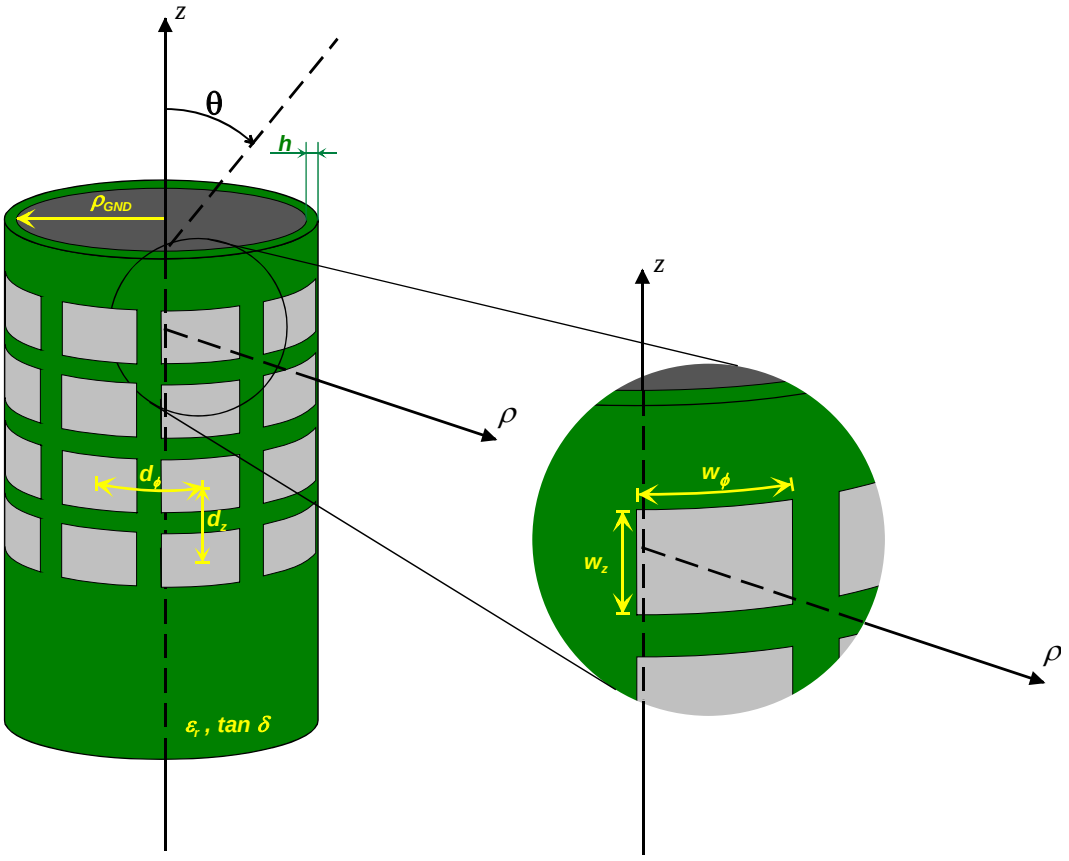

Fig. 4.6 - The geometry of the cylindrical patch array

4.2.3 TEXT FILE INTERFACE

The programs CyMPA and CyMPApat interact with the user and with each other using ASCII text files. This scheme, with all files in question is presented in Fig. 4.7.

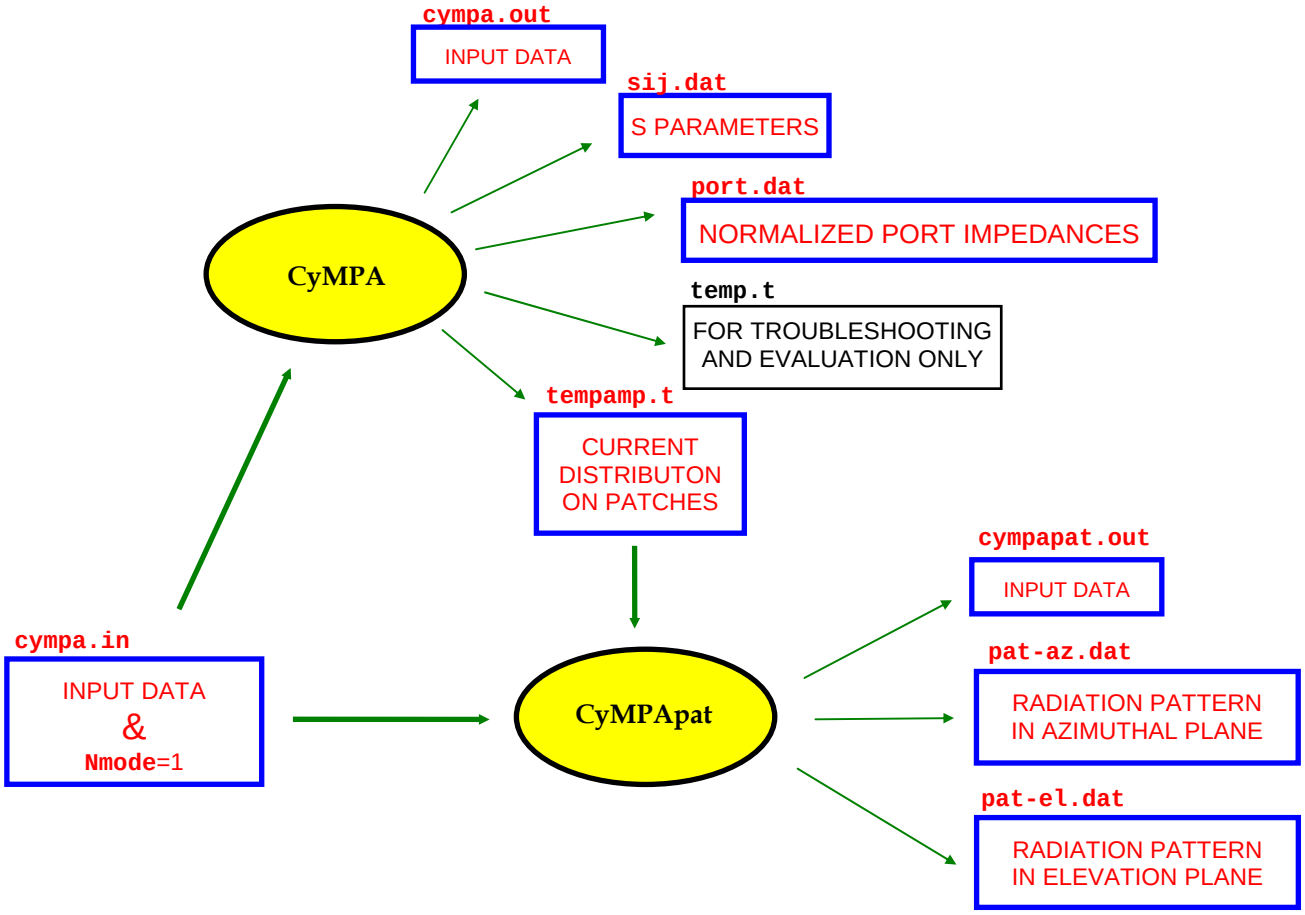

Fig. 4.7 - Procedure for calculating radiation pattern using rigorous approach

The program can calculate the following antenna characteristics:

(a) current distribution at each patch in the array

(b) input impedance of each patch in the array

(c) mutual coupling between each two patches in the array

(d) radiation pattern of the array when all mutual couplings are taken into account

(e) radiation pattern of the array without taking mutual coupling into account (fast calculations of the radiation pattern needed for making the first design of the array).

The problem of analyzing cylindrical microstrip patch arrays is split into two programs: CyMPA and CyMPApat. The CyMPA program calculates the current distribution at each patch, input impedance at each port, and S-parameters between the ports. The CyMPApat program calculates the far-field radiation pattern of the patch array. There are several possible ways of calculating the radiation pattern (see the variable Nmode in the input file '`cympa.in`'). The dominant possibility is to use calculated current distribution at each patch, which can be used for the final design of the array. Other modes of calculating radiation pattern are useful for the first design of the array. Here mutual coupling is not taken into account, and hence the current at the patches is assumed to be of the sinusoidal distribution in the

current direction and of constant distribution in the perpendicular direction. This is the common approximation because patch antennas are resonant antennas. The amplitudes of the patch current can be taken from the input file (by this we can take into account different amplitude tapers of the patch current), or they can be assumed to be equal at all patches. In the latter case the phase of the patch current can be equal at each patch, or it can be determened by the direction of the main beam. For the simplicity of application, both programs have the same input file 'cympa.in'.

As already mentioned, the most important is the file `cympa.in` which is the only interface between the layout designed by the user and both programs. The following guidelines should be followed:

- If rigorous calculation is performed and the radiation pattern is of interest, the `cympa.in` must be created and then first CyMPA and then CyMPApat must be run
- If only the current distribution, input impedance or mutual coupling are of interest then after creating `cympa.in` only the CyMPA program must be run
- If simple and fast calculation of the radiation pattern is needed, the `cympa.in` must be created and only the CyMPApat program must be run

The `cympa.in` file

The name of the input file for both CyMPA and CyMPApat programs is **cympa.in**. Each line possesses the value of several variables and short description of these variables. The input variables, which must have values when the call of the CyMPA and CyMPApat is made, are:

First line:

`Fmin, Fmax, Nfrequency` — REAL, REAL, INTEGER

Fmin and Fmax are the minimum and maximum frequency (in GHz). Nfrequency is the number of frequency points for which the array is analyzed. These values are used only when the call of the CyMPA program is made. CyMPApat program calculates the radiation pattern only for one frequency, and that frequency is Fmin. If we first calculate the patch currents at *Nfrequency* frequency points (by calling CyMPA program), then we can choose the frequency point for which we want to calculate the radiation pattern by choosing Fmin. The only condition is that the patch currents are calculated for chosen frequency point.

Second line:

R_{GND} — REAL

R_{GND} is the radius of the grounded tube (in cm).

Third line:

`Nlayer` — INTEGER

Nlayer is the number of dielecric layers.

Next *Nlayer* lines:

`h, EpsilonR, Tdelta` — REAL

Each line contains three parameters: h, EpsilonR and Tdelta which describe the thickness, the relative permitivitty and loss tangent of each dielectric layer, respectively.

Next line:

`Npatphi, Npatz` INTEGER

Npatphi and Npatz are the number of patches in the ϕ- and z-directions, respectively.

Next line:

`Npatlayer` INTEGER

Npatlayer is the number of the dielectric layer at top of which the patches are placed. In other words, patches are placed between dielectric layers *Npatlayer* and *Npatlayer*+1. If the patches are placed in the middle of some dielectric layer, an additional dielectric layer should be introduced, i.e. the considered dielectric layer should be splitted into two parts and the patches should be placed at the interface between these two dielectric layers.

Next line:

`Wpatphi, Wpatz` REAL

Wpatphi and Wpatz are the widths of the patches (in cm) in the ϕ- and z-directions, respectively.

Next line:

`Modefeed` CHARACTER

Modefeed denotes the type of the patch feeding. M or m means microstrip line feeding, C or c means coax feeding.

Next line:

`Nport` INTEGER

Nport denotes the number of ports per patch (i.e. how many port has each patch).

Next *Nport* lines:

`Feedphi, Feedz` REAL

Feedphi and Feedz determine the position of the feeding line (in cm) in the ϕ- and z-direction, respectively. Each line describes one port of the patch. This position is according to the patch center, i.e., the feeding line placed at patch center has coordinates Feedphi = Feedz = 0. If the patch is fed by the microstrip line, one value should be ±Wpatphi/2 or ±Wpatz/2, depending at which edge the patches are excited. Feedphi and Feedz also determine the polarization of the array when CyMPApat is used in the simple mode. In more details, when Feedphi = 0 current on patches is z-directed, and when Feedz = 0 current on patches is ϕ-directed. Otherwise, the current on patches is a linear combination of ϕ-directed and z-directed basic basis functions.

Next line:

`Modeexci` CHARACTER

Modeexci determines if the ports have equal excitations, both in amplitude and phase. Y or y means that the ports are equally excited, N or n means that the excitations are read at the end of the input file cympa.in.

Next line:

`Dpatphi, Dpatz` REAL

Dpatphi and Dpatz are the distances between centers of the patches (in cm) in the ϕ- and z-directions, respectively.

Next line:

`Z0, Wfeed` REAL

Z0 is the characteristic impedance of the input transmission line (either microstrip or coax line). Wfeed is the width of the input microstrip line, i.e. Wfeed is used only in the case of feeding by microstrip line. In the case of coax feeding there is no need to put the value for Wfeed.

The next six lines are needed only when the call of the CyMPApat program is made. They are:

`Phimin, Phimax, Nphi` REAL, REAL, INTEGER

The minimum and maximum angles of ϕ (in deg) in the azimuthal plane, and the number of points which are calculated in the azimuthal pattern, respectively. The azimuthal plane is defined by $\theta = 90^0$ (the coordinate system is in Fig. 1).

`Thetamin, Thetamax, Ntheta` REAL, REAL, INTEGER

The minimum and maximum angles of θ (in deg) in the elevation plane, and the number of points which are calculated in the elevation pattern, respectively.

`Phiel` REAL

The ϕ angle of the elevation plane (in deg). In other words, the elevation plane is defined by ϕ = Phiel.

`Theta0, Phi0` REAL

The values of the θ and ϕ coordinates (in deg) of the main beam, respectively. The E-field values of the radiation pattern are normalized by the amplitude of the E-field with Theta0 and Phi0 coordinates. Furthermore, Theta0 and Phi0 values are needed when Nmode=4 (see definition of the Nmode), and they are used for determining the phase correction of the current on each patch. By using this phase correction the fields from each patch are in phase in the (Theta0, Phi0) direction.

`Typepolar` CHARACTER

Typepolar denotes the type of polarization of radiation pattern. L or l means linear polarization, C or c means circular polarization.

`Nmode` INTEGER

Nmode is the mode of calculating the radiation pattern. Nmode=1 means that the radiation pattern is calculated rigorously, i.e., the results from the CyMPA program are used (the calculated current distribution for chosen frequency point, see explanation of Fmin). Nmode greater than 1 means that the radiation pattern is calculated in a simple way, i.e., mutual coupling is not taken into account in calculations of the radiation pattern. Therefore, the current on the patches is assumed of the sinusoidal distribution in the direction of the current, and of constant distribution in the perpendicular direction. When Nmode = 2 it is supposed that patch currents have equal amplitudes and phases on each patch. When Nmode = 3 amplitudes and phases of each patch current are read from the input file 'cympapat.in'. When Nmode = 4 all patches

have the same amplitude of the current. The phase is corrected in the way that contributions from all patches are in phase in the direction of the main beam, i.e., in the (theta0, phi0) direction.

The last part of the input file is used in two cases: if the ports do not have equal excitations and we want to run CyMPA program, and if we want to calculate the radiation pattern (CyMPApat program) by using the simple method and by selecting the amplitudes and phases of currents on each patch (Nmode = 3). In both cases the amplitudes and phases of the excaitation currents are read from the end of the input file cympa.in. The number of lines in the file is the same as the number of patches times number of ports (Npatphi · Npatz · Nport). Each line has 5 numbers: first two are the patch number, i.e., the number of the patch in z and ϕ direction (the patch number of the lowest most left patch is (1,1)). The third one is the number of the port of the considered patch. The fourth and the fifth number in each line are the amplitude and the phase of the excitation connected to the considered port of the patch. We can check if these last lines are correctly given by checking the description of the array given in the output files cympa.out and cympapat.out. If we are considering some other case (e.g. if the ports have equal excitations) there is no need for these input data. Therefore:

Next *Npatphi* x *Npatz* x *Nport* lines after one blank line are (if needed):

`Ipatphi, Ipatz, Iport, Amp, Phase` INTEGER, REAL

Ipatphi, Ipatz, Iport are integers which represents the coordinates of each port (coordinate Iport) connected to each patch (coordinates Ipatphi, Ipatz). For that port real numbers Amp and Phase denote the amplitude and the phase of the excitation current.

Description of the output files

There are six output files: 'cympa.out', 'cympapat.out', 'Sij.dat', 'port.dat' 'pat-az.dat' and 'pat-el.dat', and in them data about the geometry as well as the calculated values of the input impedance, S-parameters and radiation pattern in the elevation and azimuthal planes can be found.

`cympa.out` The file contains data about the input impedance of a single patch (S parameters for array case are given in Sij.dat). When constructing the array we need first to determine the parameters of a single patch like, for example, input impedance, return loss, and impedance bandwidth. The structure of the CyMPA program (and output file 'cympa.out') enables this calculations. First part of the file contains the values of the input file. Therefore the first part looks similar to the input file 'cympa.in'. The second part contains the input impedance and return loss for all calculated frequencies. Each line is for one frequency point, and it has four values: frequency (in GHz), normalized input impedance (real and imaginary part) and return loss (in dB). The calculated input impedance is normalized by the characteristic impedance of the feeding transmission line Z0 (the value of Z0 is given in the file 'cympa.in').

`cympapat.out` The file contains data about the array geometry. The first part of the file contains the values of the input file. Therefore the first part looks similar to the input file 'cympa.in'. The second part describes the array which is analyzed. It is a list of the all patch elements in the array with their coordinates and amplitude and phase of the patch currrent. First two columns are the patch number in the z and ϕ direction. The third column is the number of the basis function on the considered patch. The forth and fifth columns are the z and ϕ coordinate of the patch. The sixth and seventh columns are the amplitude and phase (in deg) of the considered basis function, respectively.

Sij.dat The file contains the calculated S-parameters. The file is in the Touchstone format, i.e., by this file it is possible to connect CyMPA and Touchstone programs. The first line is a specification line: '# MHz S DB R' and at the end of the line there is a value of the normalization impedance. MHz means that the frequency values are in MHz, DB means that S-parameters are written in the dB-angle format. Other lines in the file are the S-parameters for different frequencies. If we have one port (one patch) then each line contains frequency, $|S_{11}|$ in dB, and angle of $S_{11,}$ respectively. If the case of two ports (two patches) each line contains frequency, $|S_{11}|$ in dB, angle of S_{11}, $|S_{21}|$ in dB, angle of S_{21}, $|S_{12}|$ in dB, angle of S_{12}, $|S_{22}|$ in dB, and angle of S_{22}, respectively. In the case of *N* ports each frequency is described with *N* lines, each containing $|S_{i1}|$ in dB, angle of S_{i1}, $|S_{i2}|$ in dB, angle of $S_{i2,}$ etc. Frequency is written at the beginning of the first of *N* lines.

port.dat The file contains the calculated port impedances for each port. For each frequency point port impedances are given in the form real and imaginary part. The values of port impedances are normalized, i.e. port impedances are divided by Z0.

pat-az.dat The file contains the field values in the azimuthal plane (the azimuthal plane is defined by $\theta=90^0$). The input values of variables Phimin, Phimax and Nphi determine the ϕ values in the azimuthal plane for which the radiation pattern is calculated. The field values are normalized with the field value with Theta0 and Phi0 coordinates which are defined in the input file. The first and second columns are the θ and ϕ coordinates (in deg) for which the radiation pattern is calculated. If the chosen type of polarization is linear (parametar Typepolar in the input file), then the third and the fourth columns are the normalized θ- and ϕ -components of the electric field, respectively. If the chosen type of polarization is circular, then the third and the fourth columns are the normalized right-hand circular polarization (RHCP) and left-hand circular polarization (LHCP) components of the electric field, respectively. The RHCP and LHCP components are calculated by using eq. (20).

pat-el.dat The file contains the field values in the elevation plane which is defined by ϕ=Phiel (the value of Phiel is defined in the input file). The input values of variables Thetamin, Thetamax and Ntheta determine the θ values in the elevation plane for which the radiation pattern is calculated. The field values are normalized with the field value with coordinates Theta0 and Phi0 which are defined in the input file. The first and second columns are the θ and ϕ coordinates (in deg) for which the radiation pattern is calculated. If the chosen type of polarization is linear (parametar Typepolar in the input file), then the third and the fourth columns are the normalized θ- and ϕ -components of the electric field, respectively. If the chosen type of polarization is circular, then the third and the fourth columns are the normalized right-hand circular polarization (RHCP) and left-hand circular polarization (LHCP) components of the electric field, respectively. The RHCP and LHCP components are calculated by using eq. (20).

4.2.4 GRAPHICAL USER INTERFACE

The CympaWin is designed as a helper application to make it easier for the users to interact with CyMPA and CyMPApat. These programs are designed for the command line environment, to ensure the compatibility with all platforms having the FORTRAN compiler, compiler of the language in which both programs are originally written. In such an environment, the antenna design input data must be entered manually using some ASCII editor into file cympa.in.

The CympaWin is a Microsoft Windows® based program and enables the user to create input files for CyMPA and CyMPApat with a click of a mouse, avoiding exhausting procedure of careful editing of input data into cympa.in files directly.

Note: The Cympa and CympaPat should still be executed from the command line prompt. CympaWin executes them from MS - DOS prompt automatically.

Is the installation of CympaWin **complicated?**

Actually, there is no installation procedure. Simply copy the CympaWin executable file CYMPAWIN.EXE, and calculation programs CYMPA.EXE and CYMPAPAT.EXE to the directory of your choice, and make shortcut on the desktop pointing to the CympaWin program icon if you like. After starting the CympaWin, you should have no problems designing your first antenna configuration and running calculations.

Troubleshooting: *In case CyMPA or CyMPApat would not start, try running them directly from the command line within the program directory. Use the same configuration data that was generated by CympaWin (it is in the 'cympa.in' file) and watch for the program output screen for any problem. The computer should be at least 386 with 16 Mb RAM and Windows 95 or later installed.*

How does CympaWin **work?**

As already mentioned, the Cympa and CympaPat use input file sympa.in to get the configuration data from the user and they generate output files with calculation results. Configuration and output file names are same for each program run, so new calculations overwrite previous results. This is still the case, but now there is an interface between the user and those files.

Configuration for which calculations will be performed is saved in the specified directory under the name selected through the standard dialog box. It is not possible to run calculations if the configuration was changed without saving it first. The application title bar indicates the file name (You will note '*' appended to the end of the name if file was changed but not saved).

This filename will be used as the base name for all results generated and stored for the particular configuration. Only the file name extensions will be different. CympaWin configuration file extension is 'cin', and the selected configuration file is copied into the 'cympa.in' file in the application working directory before starting the Cympa and/or CympaPat program.

After appropriate program is executed, calculated results are copied to the configuration file directory. Next time, when calculation will be run for different configuration, the previous results should be intact, unless the same files name and directory is used for the configuration file.

One can also check the previous results without running the calculations again. When the configuration name is selected, CympaWin will enable View submenu items if previous output results were found in the selected directory. If new results are needed, configuration should be edited, then saved, and Cympa and/or CympaPat programs should be executed again. New results could than be checked under the View menu. Note that result will not be shown after calculation execution until View menu is selected.

Input and output files

The configuration file name could be considered as a project name, since all files will have the same base name and specific extensions. Of course, the CyMPA and CyMPApat both generate fixed file names, but those are in the program directory and will be saved after calculation into the configuration directory as follows:

pat-az.dat	will be copied as project_name.paz, CympaPat execution result containing field values in the azimuthal plane
pat-el.dat,	will be copied as project_name.pel, CympaPat execution result containing field values in the elevation plane
temp2.t	will be copied as project_name.sij, CyMPA execution result containing the patch mutual coupling and input impedance information

This three files contain sufficient information about the simulation run.

Also the various temporary files will be generated during the program run within the program directory. Some of them are used for status information and synchronization between the Windows® and DOS application and are deleted before or after the program execution.

The user interface description

The CympaWin is designed as the standard Windows SDI (Single Document Interface). The imperative was to maintain the look and feel of standard Windows applications to minimize the learning curve while keeping things as simple as possible.

Although no program could be made bullet proof against the user input errors, we tried to minimize problems by forcing user to enter at least correct type of parameters, and by not allowing saving configuration with empty values.

The CympaWin is menu oriented with the Toolbars duplicating some more frequent operations. Submenu items are logically grouped, and disabled ('grayed') if operation is not possible within the current context. Standard dialog boxes are used for the file operations.

Window 1
File | New or File | Open should be the first user action because most of the other operations are not possible until the configuration name is known. As the figure Window 1 shows, the configuration file 'Test.cin' is already loaded and some of the toolbars are enabled.

Window 2
Configuration creating, editing, and viewing is realized with the Page Control Dialog Box (Style Sheets) as shown in figure Window 2. Groups of parameters are placed at the same page if they belong together logically.

Window 3
Any empty parameter will cause the error message box to pop up when user tries to leave the empty control. It is only possible to leave the control without filling correctly by selecting the Cancel button.

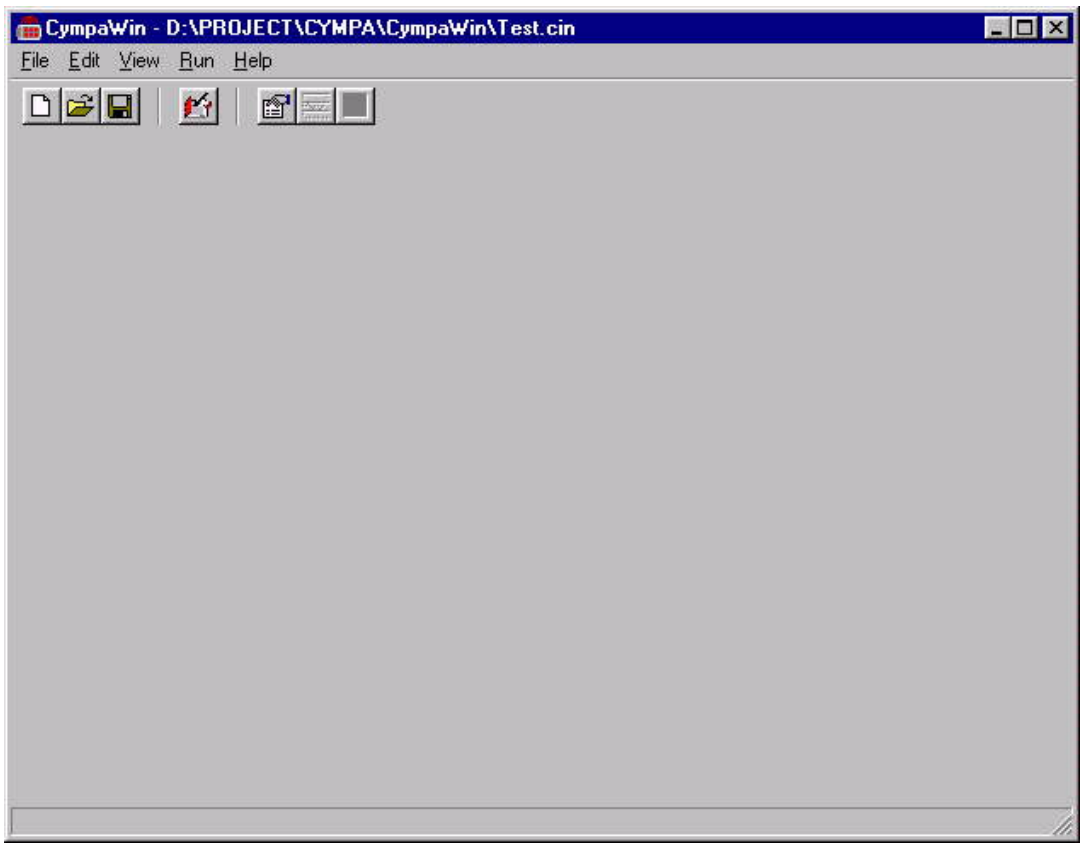

Window 1

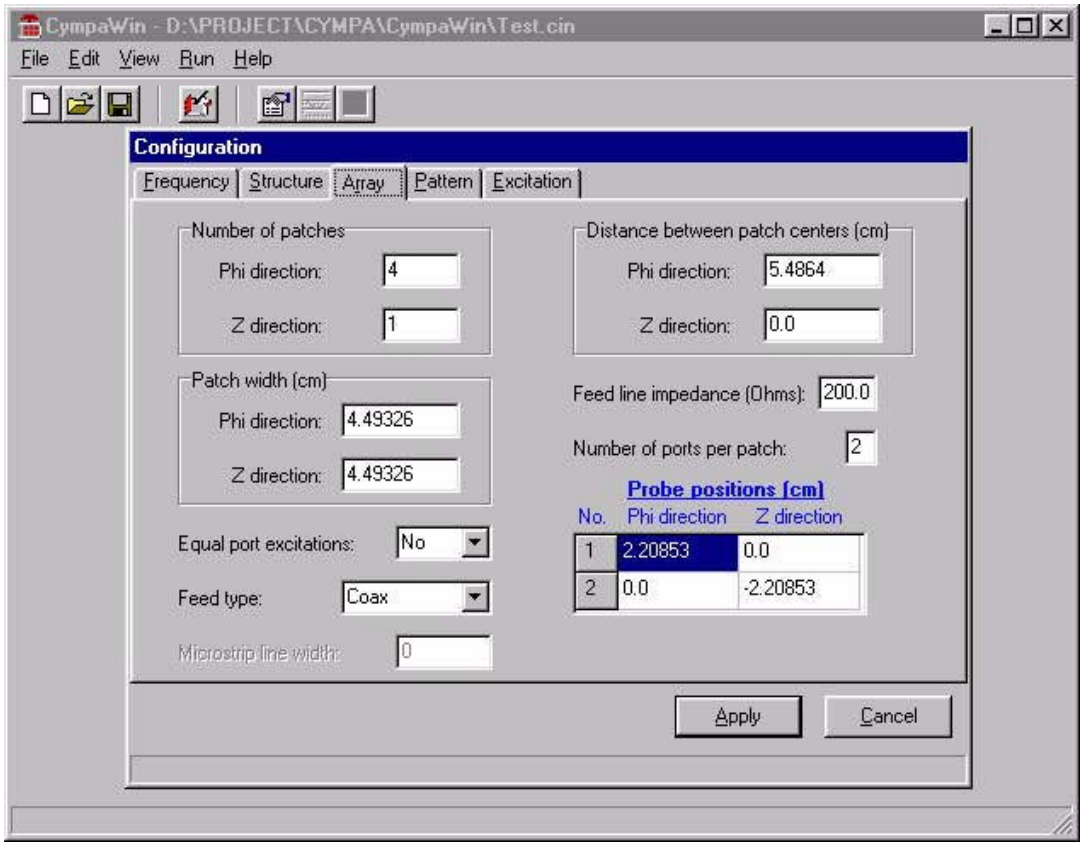

Window 2

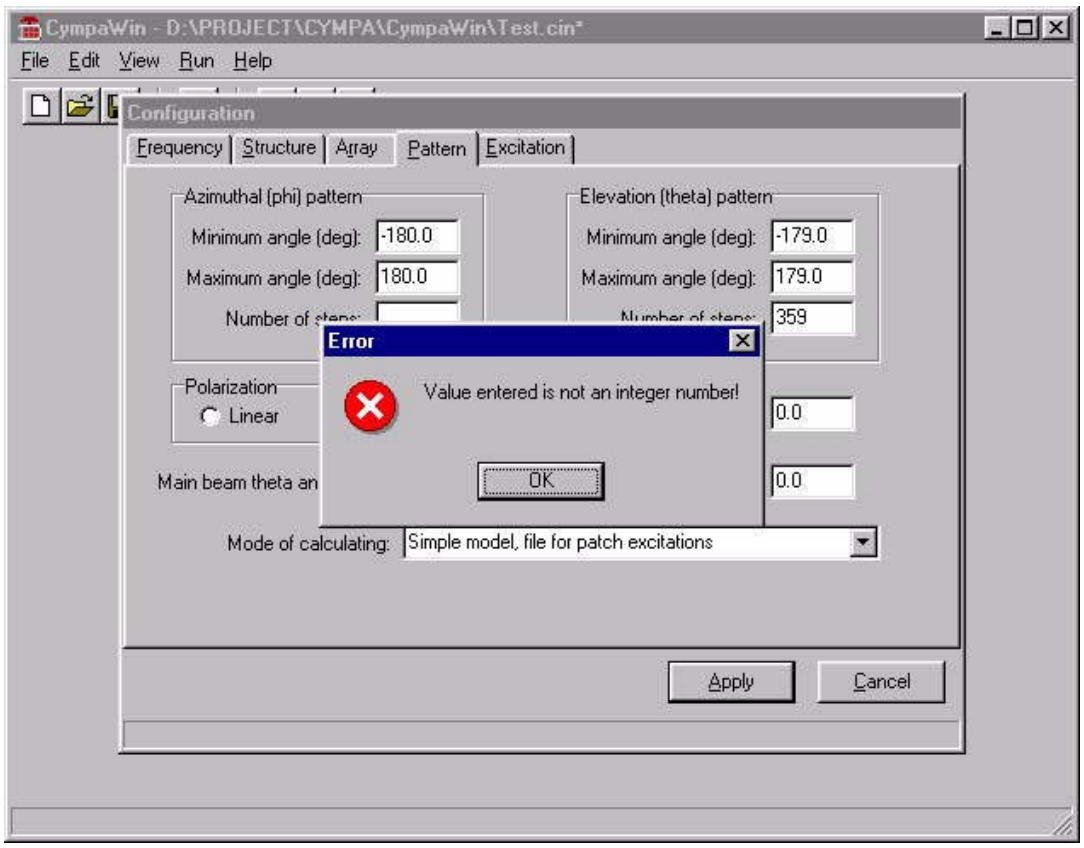

Window 3

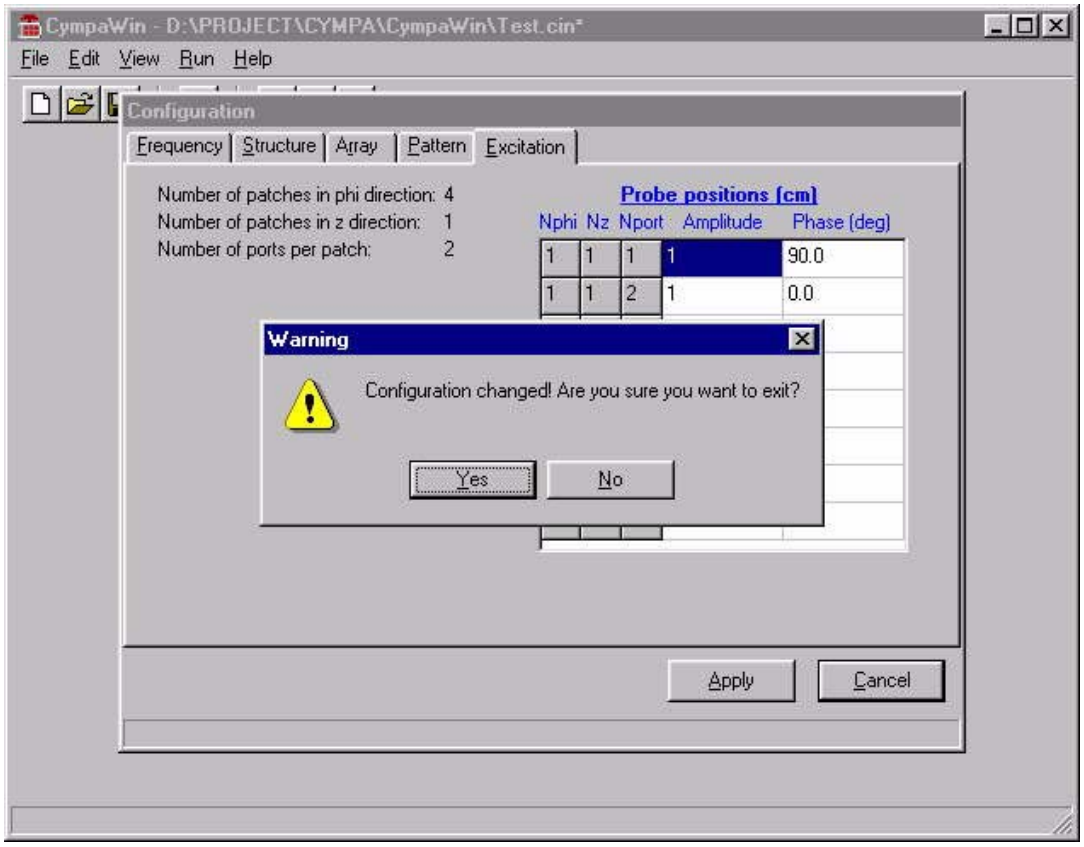

Window 4

Window 4
The application will not ask for confirmation when Cancel button is pressed because it is always possible to go back to editing. Confirmation will be requested if user tried to leave the program without saving file which has been changed.

Window 5
Tables are automatically resized when parameters that determine the number of rows are changed. Columns are filled with information based on the row numbers where possible, so the user is spared of entering repetitive information. Scroll bars are shown when table does not fit the page control size.

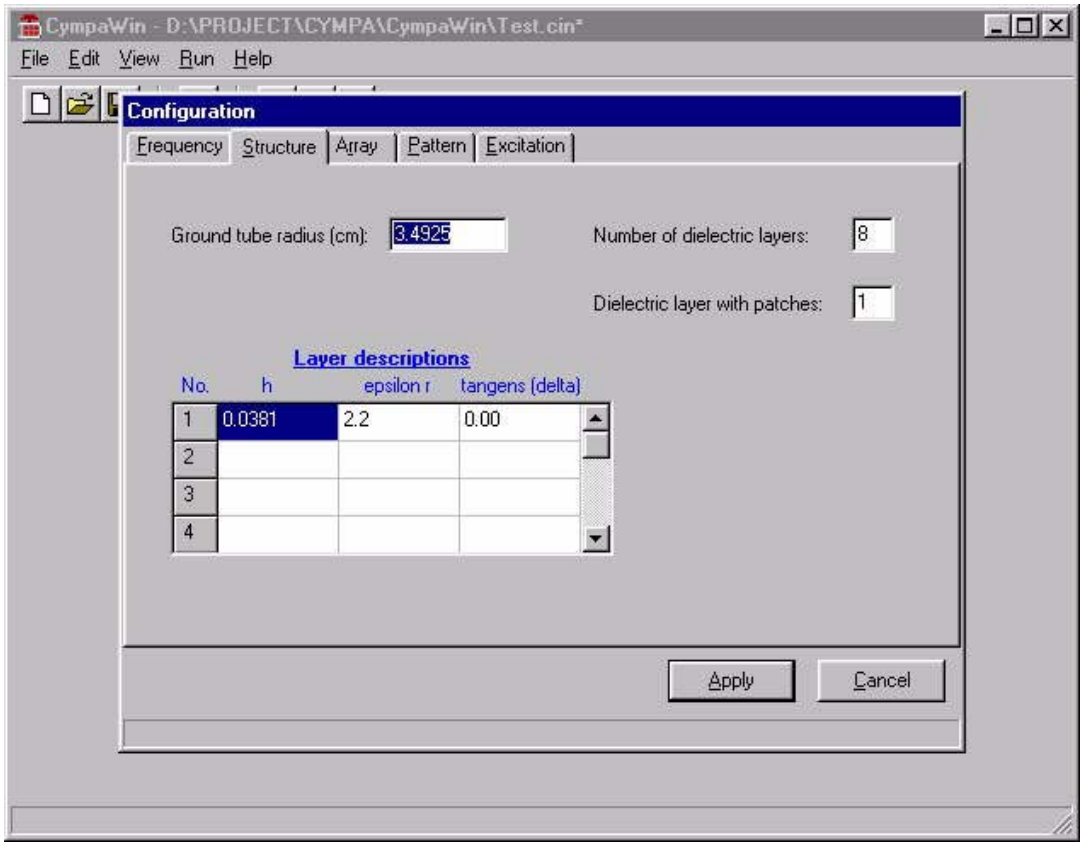

Window 5

Run menu contains two submenu items:

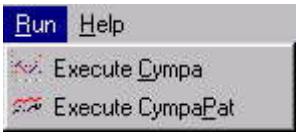

Cympa and CympaPat applications are executed as minimized DOS boxes, and user could maximize them and watch the program output as he / she would do within the command line environment.

After corresponding application is properly executed and output files are generated, View submenu items are enabled:

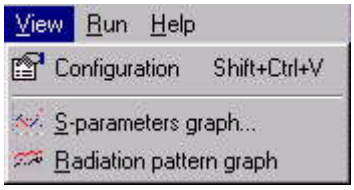

4.3 BENCHMARKS

4.3.1 RADIATION PATTERN OF 4x4 MICROSTRIP ARRAY

As first example, the radiation pattern of the 4x4 array depicted in Fig. 4.8 is calculated. The data describing structure and properties of this array are presented in Table 4.8. Here, a comparison between simple and rigorous approach will be given. The comparison with measurements is also presented.

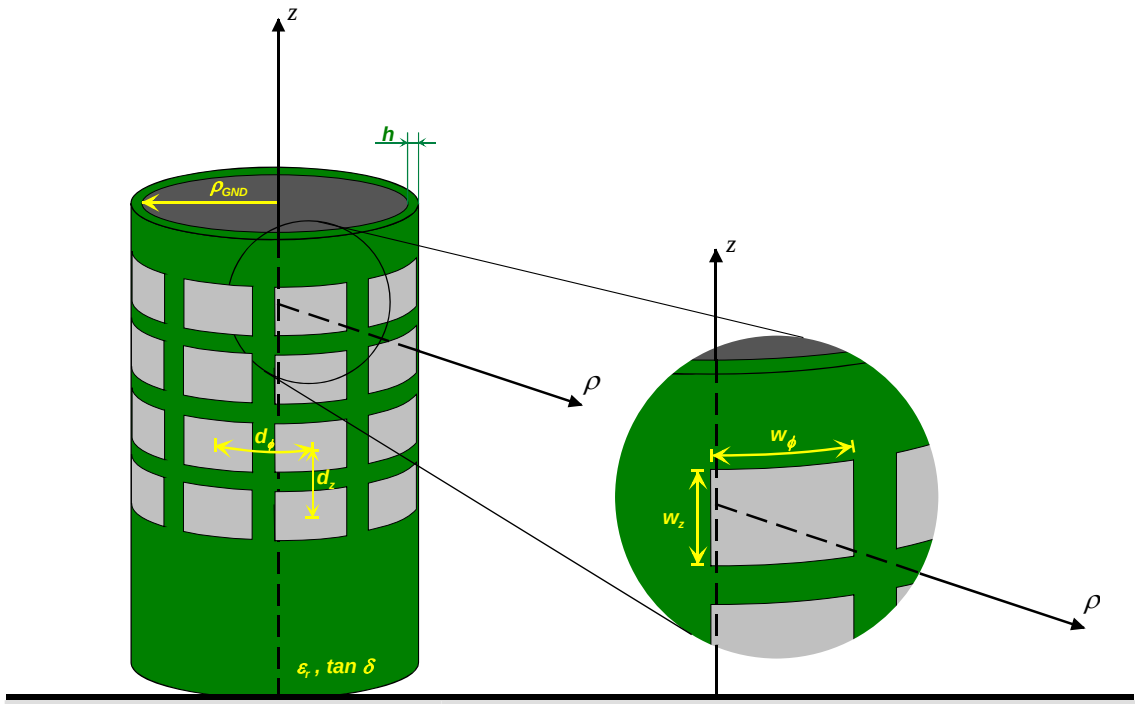

Fig. 4.8 - The layout of 4x4 patch array printed on cylindrical substrate

ITEM	PARAMETERS	DESCRIPTION
frequency	16.2 GHz	frequency at which the simulation is performed
radius of the grounded tube	ρ_{GND} = 7.6 cm	radius of the grounded tube
parameters of dielectric slab	h = 0.254 mm ε_r = 2.94 δ = 0.0015	thickness relative permittivity loss tangent
array element dimensions	w_ϕ = 0.72 cm w_Z = 0.5 cm	width of the patch in ϕ direction width of the patch in z direction
coaxial probe feed position, related to patch center	ϕ_{FEED} = 0.0 cm z_{FEED} = 0.1 cm Z_0 = 50 Ω	in ϕ direction in z direction characteristic impedance
distance between patch centers	d_ϕ = 1.5 cm d_z = 1.5 cm	in ϕ direction in z direction
main beam direction (broadside)	$\Theta_0 = 90^0$ $\Phi_0 = 0^0$	

Table 4.3 - Properties of the 4x4 microstrip patch array printed on the cylindrical substrate

Radiation pattern calculations procedure when using **simple approach** will follow the diagram in Fig. 4.9. In order to obtain radiation pattern rigorously, CyMPA program must be applied to determine rigorous current distributions on patches before calculating radiation pattern. In that case, procedure in Fig. 4.10 will be applied.

Note: **`cympa.in`** is the filename of the input file for both, CyMPA and CyMPApat programs

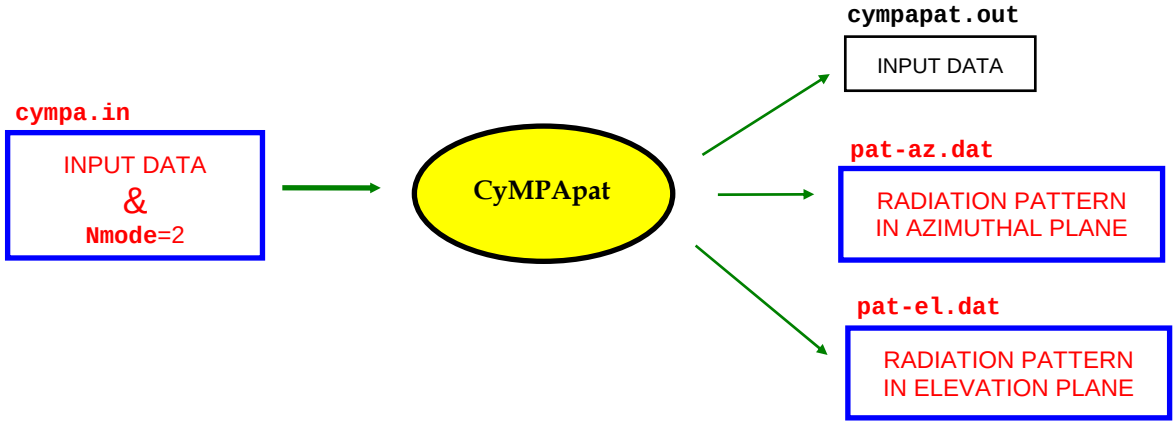

Fig. 4.9 - Procedure for calculating radiation pattern using simple approach

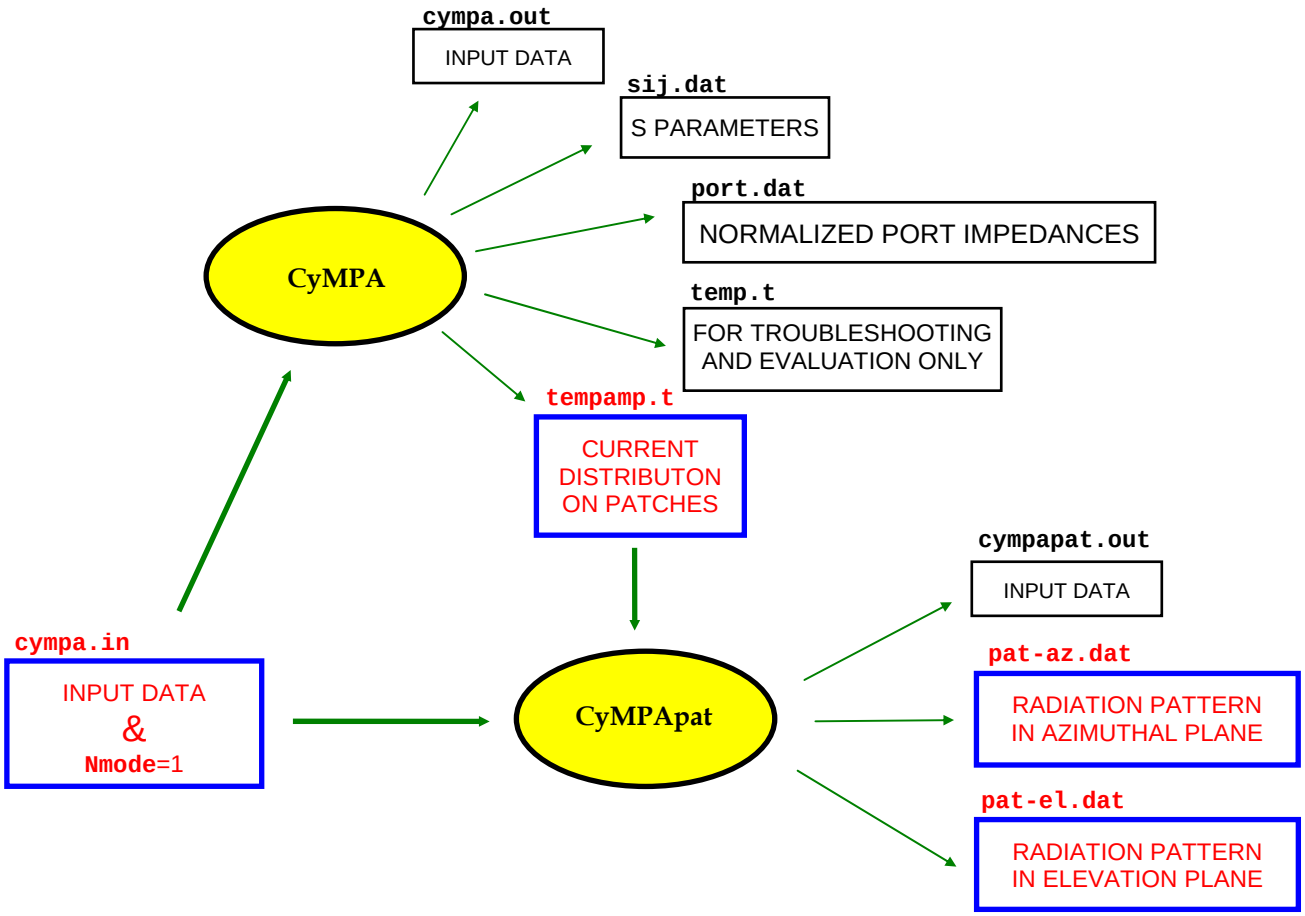

Fig. 4.10 - Procedure for calculating radiation pattern using rigorous approach

The input file "**`cympa.in`**" for this case is shown in Fig 4.11:

```
  16.2      16.2      1          ! Frequency (GHz)
  7.6                            ! Ground tube and patch radius (cm)
  1                              ! Number of dielectric layers
  0.0254   2.94      0.00        ! h, epsilon_r, tangent (delta)
  1                              ! Die. Layer at top of which patches are placed
  4           4                  ! Number of patches in phi/z direction
  0.72      0.5                  ! Patch width in phi and z direction (cm)
  C                              ! feed type (m - microstrip, c -coax)
  1                              ! Number of ports per patch
  0.0       0.1                  ! Feed position in phi and z direction (cm)
  Y                              ! Equal port excitation? (Y - yes, N - no)
  1.5       1.5                  ! Distance between patch centers
  50.0                           ! Characteristic impedance of the feed line
 -180.0     180.0     361        ! Azimuthal pattern
  1.0       179.0     179        ! Elevation pattern
  0.0                            ! Phi angle of the evaluation pattern
 90.0       0.0                  ! Theta and phi angle of the main beam
  L                              ! Polarization (L - linear, C - circular)
  1                              ! Mode of calculating the radiation pattern
```

Fig. 4.11 - Input file for CyMPA *and* CyMPApat *respectively, for applying rigorous mode. If simple mode is applied, red numbers can be of arbitrary values and blue number must be* **2**

```
Radius of the ground tube and the patch (cm)          7.6000
Number of dielectric layers (substrates)              1
1. layer: h, epsilon_r, tangent (delta)               0.0254      2.9400      0.0000
Number of layer at which patches are placed           1
Number of patches in phi/z direction                  4           4
Patch width in phi and z direction (cm)               0.7200      0.5000
Feed type (m - microstrip, c - coax)                  C
Number of ports per patch                             1
Probe coordinate in phi and z direction (cm)          0.0000      0.1000
Equal port excitations? (Y - yes, N - no)
Distance between patch centers in phi/z (cm)          1.5000      1.5000
Characteristic impedance of the feed line            50.0000
 Azimuthal pattern:
 minimum, maximum and number of points              -180.00      180.00     361
 Elevation pattern:
 minimum, maximum and number of points                 1.00      179.00     179
Phi angle of the elevation pattern (deg)              0.0000
Theta and phi angle of pattern maximum (deg)         90.0000      0.0000
Polarization (L - linear, C - circular)               L
Mode of calculating radiation pattern                 1
The highest-order mode in Fourier series              51

Frequency (GHz)                                       16.2000

        Element            Coordinates        Amplitude     Phase
    phi     z    b.f.   phi(deg)       z(cm)

     1      1      1    -16.9061     -2.2500      0.0737    127.6275
     1      1      2    -16.9061     -2.2500      0.0012    -13.6385
     1      1      3    -16.9061     -2.2500      0.0011    125.7930
     1      1      4    -16.9061     -2.2500      0.0095    139.5920
     1      1      5    -16.9061     -2.2500      0.0022    -40.2884
     1      1      6    -16.9061     -2.2500      0.0019    139.6480
     1      2      1    -16.9061     -0.7500      0.0784    126.9456
     1      2      2    -16.9061     -0.7500      0.0010     -7.8059
     1      2      3    -16.9061     -0.7500      0.0012    125.2970
     1      2      4    -16.9061     -0.7500      0.0093    138.6641
     :      :      :        :            :           :         :
```

Fig. 4.12 - **`cympa.out`** *file, generated by* CyMPA *when* **`cympa.in`** *from Fig. 4.11 is used*

In order to calculate radiation pattern rigorously, the CyMPA routine was run to calculate the patch currents. Then, CyMPApat routine was run to calculate the radiation pattern by using the rigorous approach. In order to calculate the radiation pattern by using the simple approach the mode 2 instead of 1 is selected (see Fig. 4.11).

The output file "cympapat.out" for the rigorous way of calculating far field is shown in Fig.4.12.

After running CyMPA, CyMPApat must be run to obtain radiation patterns in azimuthal and elevation planes (see Fig. 4.10). A few lines from the file '**pat-az.dat**' around $\phi = 0$ are:

```
    :          :          :          :
90.0000    -5.0000    -0.9892   -40.0183
90.0000    -4.0000    -0.6327   -41.5621
90.0000    -3.0000    -0.3557   -43.7582
90.0000    -2.0000    -0.1580   -47.0659
90.0000    -1.0000    -0.0395   -52.9589
90.0000     0.0000     0.0000  -200.0000
90.0000     1.0000    -0.0395   -52.9589
90.0000     2.0000    -0.1580   -47.0659
90.0000     3.0000    -0.3557   -43.7582
90.0000     4.0000    -0.6327   -41.5621
90.0000     5.0000    -0.9892   -40.0183
    :          :          :          :
```

The calculated radiation patterns in the azimuthal and elevation plane, obtained both by rigorous and simple method, are plotted in the Fig. 4.13. For comparison the measured results are also given (measured results are taken from [16]). It is interesting to notice that there is no big difference between the rigorous and simple model for calculating the radiation pattern for this relatively small array.

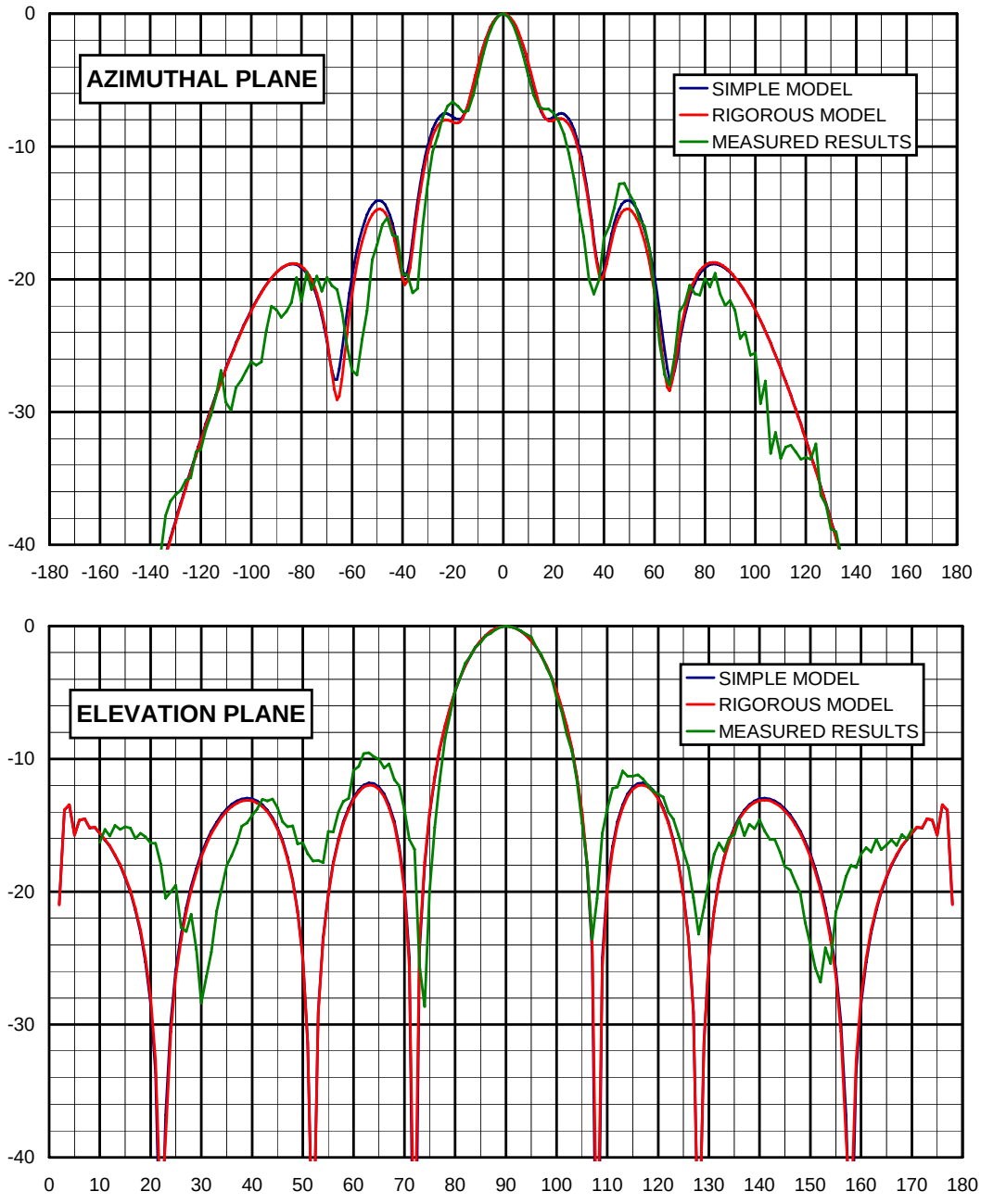

Fig. 4.13 - Calculated and measured radiation patterns for 4x4 microstrip array

4.3.2 MUTUAL COUPLING OF PATCHES IN E AND H PLANES

As second example we calculated S_{21} parameter between two patches in 1.5 GHz band. Both, E- and H-plane coupling will be analyzed and presented.

The geometry of two patches coupled in E-plane is shown in Fig. 4.14. The parameters of patches and dielectric slab are given in Table 4.4.

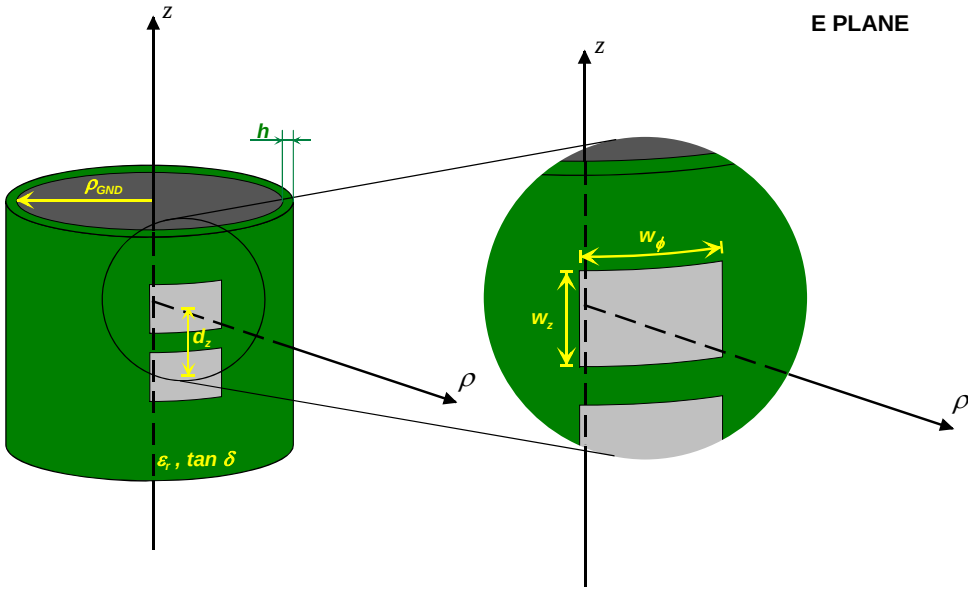

Fig. 4.14 - Geometry of two patches printed in z direction, coupled in E-plane

ITEM	PARAMETERS	DESCRIPTION
frequency	1.46-1.53 GHz	frequency band in which the simulation is performed
radius of the grounded tube	ρ_{GND} = 5 cm	radius of the grounded tube
parameters of dielectric slab	h = 0.762 mm ε_r = 2.32	thickness relative permittivity
array element dimensions	w_ϕ = 11 cm w_Z = 6.5 cm	width of the patch in ϕ direction width of the patch in z direction
coaxial probe feed position, related to patch center	ϕ_{FEED} = 0.0 cm z_{FEED} = 1.6 cm Z_0 = 50 Ω	in ϕ direction in z direction characteristic impedance
distance between patch centers	d_z = 12.5 cm	in z direction

Table 4.4 - Properties of patches printed on cylindrical substrate in z direction (E plane)

The calculation procedure needed to solve this problem is depicted in Fig. 4.15.

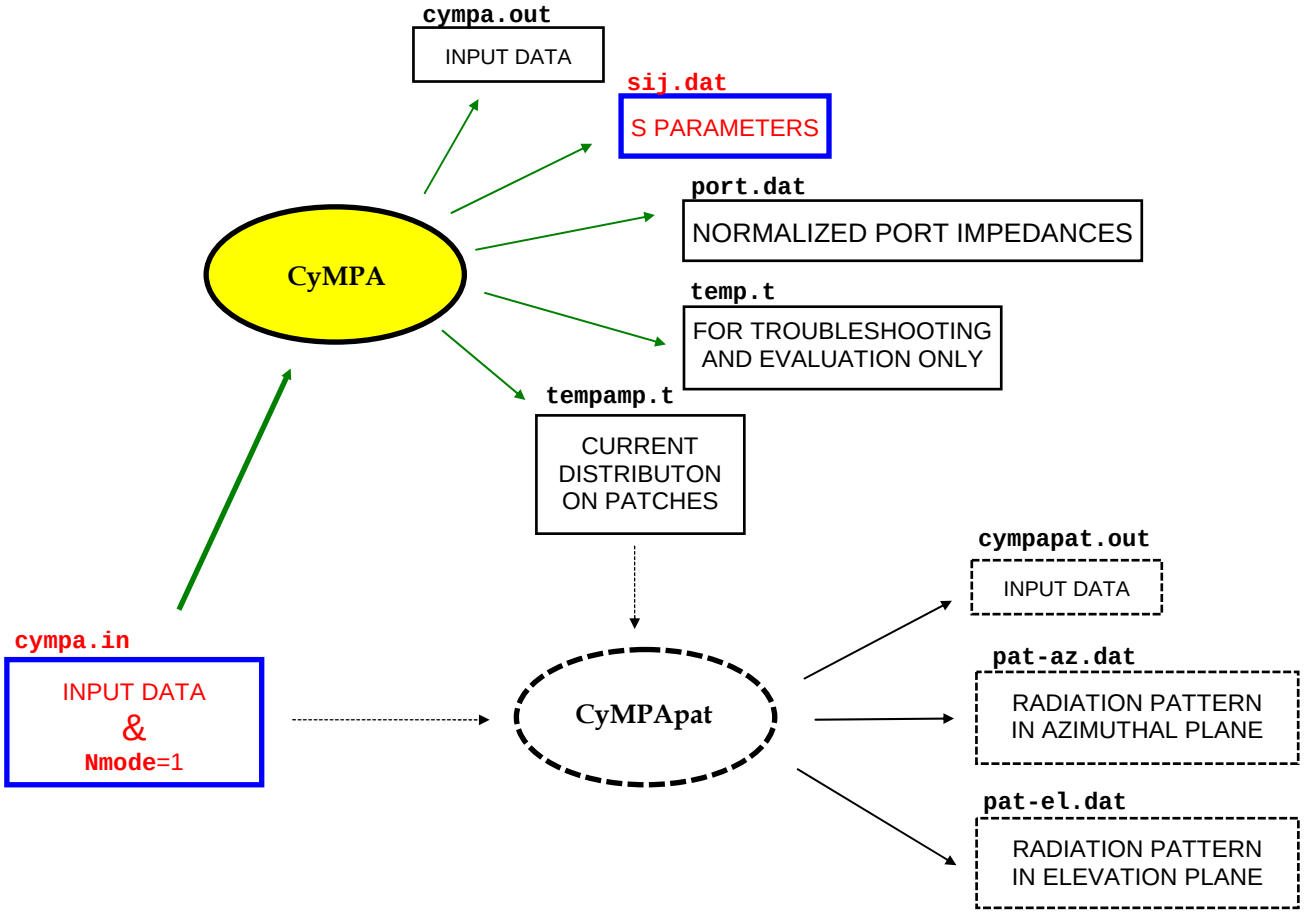

Fig. 4.15 - Procedure for calculating mutual coupling

```
  1.46      1.53      15            ! Frequency (GHz)
  5.0       5.0762                  ! Ground tube and patch radius (cm)
  1                                 ! Number of dielectric layers
  0.0762    2.32       0.00         ! h, epsilon_r, tanges (delta)
  1                                 ! Die. layer at top of which patches are placed
  1         2                       ! Number of patches in phi/z direction
  11.0      6.50                    ! Patch width in phi and z direction (cm)
  C                                 ! Feed type (M - microstrip, C - coax)
  1                                 ! Number of ports per patch
  0.0       1.6                     ! Feed position in phi and z direction (cm)
  Y                                 ! Equal port excitation (Y - yes, N - no)
 12.0      12.5                     ! Distance between patch centers
 50.0                               ! Characteristic impedance of the feed line
 -180.0       180.0     361         ! Azimuthal pattern
  1.0         179.0     179         ! Elevation pattern
  0.0                               ! Phi angle of the evelation pattern
 90.0      0.0                      ! Theta and phi angle of the main beam
  L                                 ! Polarization (L - linear, C - circular)
  1                ! Mode of calculating the radiation pattern
```

Fig. 4.16 - The input file `cympa.in` *for calculating mutual coupling between two patches in E plane. In order to obtain mutual coupling of patches in H plane, values 1 and 2 must be exchanged in the line marked red.*

The input file '**`cympa.in`**' for E-plane coupling is shown in Fig. 4.16. In order to obtain the H-plane coupling between patches, as shown in Fig. 4.17, the number of patches in ϕ direction will be 2 and in z direction 1. Here, the distance between patch centers d_ϕ is equal 12.5 cm.

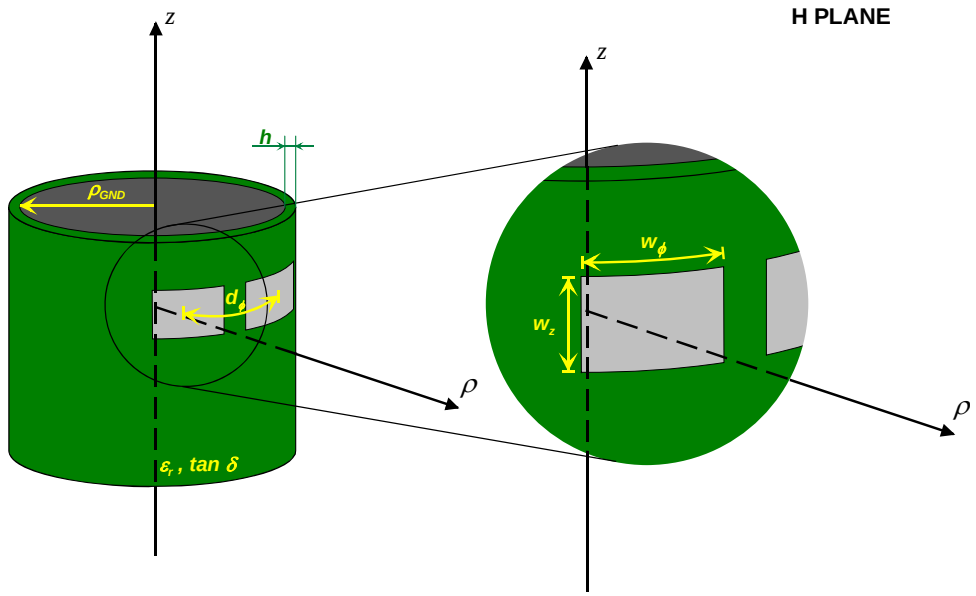

Fig. 4.17 - The geometry of patches for calculation of mutual coupling in H plane

```
# MHz S DB R   50
  1460.0    -0.68  140.95  -36.02  142.44  -36.02  142.44   -0.68  140.95
  1465.0    -0.89  137.85  -33.93  135.47  -33.93  135.47   -0.90  137.85
  1470.0    -1.22  133.87  -31.62  126.65  -31.62  126.65   -1.22  133.87
  1475.0    -1.74  128.62  -29.09  115.13  -29.09  115.13   -1.75  128.62
  1480.0    -2.64  121.54  -26.37   99.69  -26.37   99.69   -2.65  121.55
  1485.0    -4.33  111.89  -23.61   78.58  -23.61   78.58   -4.35  111.94
  1490.0    -7.97   99.30  -21.20   50.06  -21.20   50.06   -8.00   99.46
  1495.0   -19.53   91.42  -19.90   14.38  -19.90   14.38  -19.58   92.43
  1500.0   -12.94 -126.65  -20.37  -23.49  -20.37  -23.49  -12.92 -127.11
  1505.0    -6.19 -139.79  -22.40  -56.44  -22.40  -56.44   -6.19 -139.97
  1510.0    -3.55 -151.43  -25.20  -81.51  -25.20  -81.51   -3.55 -151.52
  1515.0    -2.25 -160.03  -28.13  -99.73  -28.13  -99.73   -2.25 -160.08
  1520.0    -1.54 -166.31  -30.92 -113.05  -30.92 -113.05   -1.54 -166.35
  1525.0    -1.11 -171.01  -33.50 -123.02  -33.50 -123.02   -1.11 -171.03
  1530.0    -0.84 -174.62  -35.85 -130.70  -35.85 -130.70   -0.84 -174.64
```

Fig. 4.18 - The output file `sij.dat` *containing the S parameters of coupling between two patches in E plane*

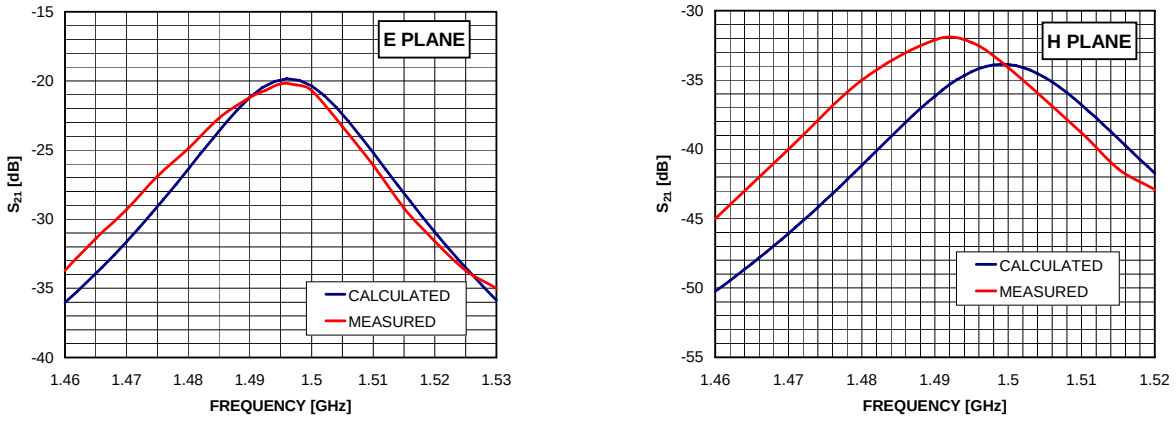

Fig. 4.19 - Calculated and measured mutual coupling coefficients in E and H plane

The S-parameters for the E plane coupling are given in the file '`Sij.dat`', shown in Fig. 4.18. Fig. 4.19 shows the comparison between measured and calculated S21 coefficient as a function of frequency. The measureed results are taken from [17].

4.3.3 PATCH ARRAY FOR CIRCULAR POLARIZATION

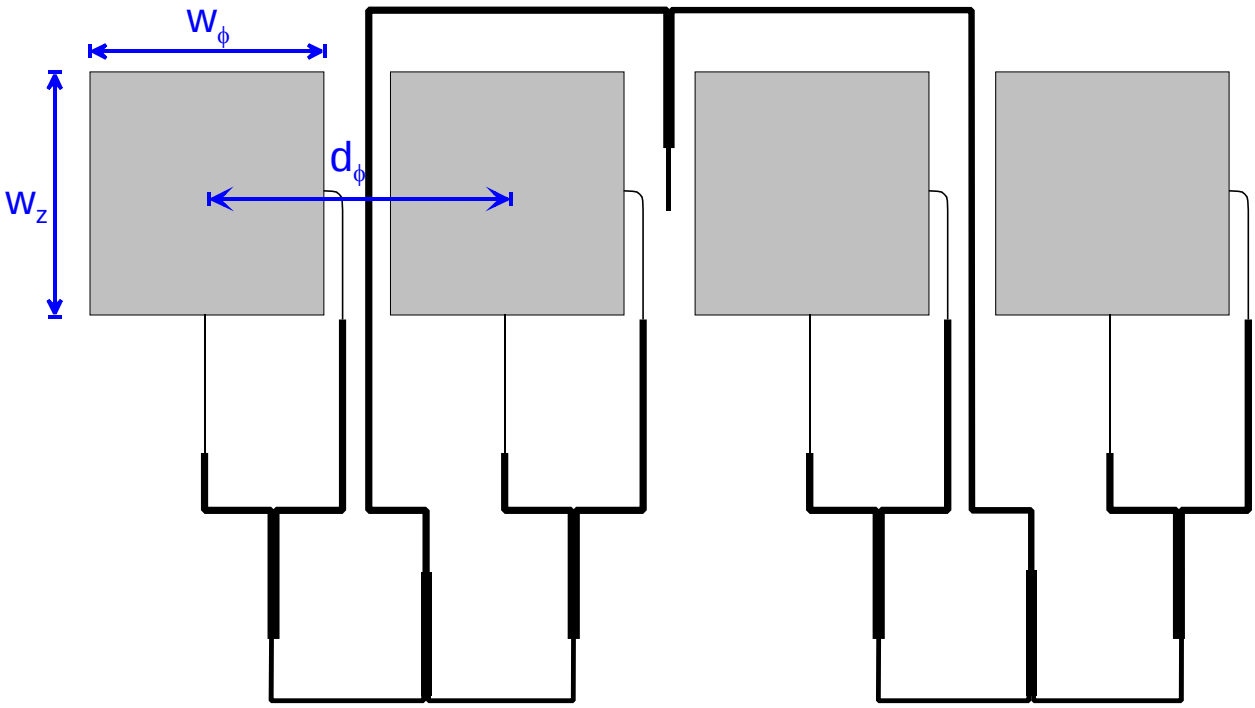

Fig. 4.20 - 1x4 squared patch array for circular polarization

We calculated the radiation pattern of 1x4 array of squared patches fed by two microstrip transmission lines. One transmission line is for excitation of the ϕ-direceted current, and the other one is for excitation of the z-directed current. In order to obtain the right-hand circular polarization (RHCP) there is a phase shift of 90^0 of the ϕ-direceted current obtained by a $\lambda/4$ delay line. The parameters fr this simulation are presented in Table 4.5.

ITEM	PARAMETERS	DESCRIPTION
frequency	2.2355 GHz	frequency at which the simulation is performed
radius of the grounded tube	ρ_{GND} = 3.49 cm	radius of the grounded tube
parameters of dielectric slab	h = 0.381 mm ε_r = 2.2	thickness relative permittivity
array element dimensions	w_ϕ = 4.49 w_Z = 4.49	width of the patch in ϕ direction width of the patch in z direction
microstrip line feed, position related to patch center	ϕ_{FEED1} = 0.0 cm z_{FEED1} = -2.246 cm ϕ_{FEED2} = 2.246 cm z_{FEED2} = 0.0 cm Z_0 = 200 Ω	in ϕ direction, first feed point in z direction, first feed point in ϕ direction, second feed point in z direction, second feed point characteristic impedance
distance between patch centers	d_ϕ = 5.49 cm	in ϕ direction

Table 4.5 - Properties of patches printed on cylindrical substrate in z direction (E plane)

The program execution flow is equal as in first example and is shown in Fig. 4.10. The corresponding input file '`cympa.in`' is shown in Fig. 4.21.

```
 2.2355    2.2355      1          ! Frequency (GHz)
 3.4925                           ! Ground tube radius (cm)
 1                                ! Number of dielectric layers
 0.0381    2.2         0.00       ! h, epsilon_r, tanges(delta)
 1                                ! Die. layer at which patches are placed
 4         1                      ! Number of patches in phi/z direction
 4.49326   4.49326                ! Patch width in phi and z direction (cm)
 M                                ! Feed type (M - microstrip, C - coax)
 2                                ! Number of ports per patch
 2.20853   0.0                    ! Probe position in phi and z direction (cm)
 0.0      -2.20853                ! Probe position in phi and z direction (cm)
 N                                ! Equal port excitations? (Y - yes, N -no)
 5.4864    0.0                    ! Distance between patch centers
 200.0     0.0348                 ! Characteristic impedance of the feed line
-180.0       180.0     361        ! Azimuthal pattern
-179.0       179.0     359        ! Elevation pattern
 0.0                              ! Phi angle of the evelation pattern
90.0      0.0                    ! Theta and phi angle of the main beam
 C                                ! Polarization (L - linear, C - circular)
 1                                ! Mode of calculating the radiation pattern

 1     1      1      1.0000        90.0000
 1     1      2      1.0000         0.0000
 2     1      1      1.0000        90.0000
 2     1      2      1.0000         0.0000
 3     1      1      1.0000        90.0000
 3     1      2      1.0000         0.0000
 4     1      1      1.0000        90.0000
 4     1      2      1.0000         0.0000

 Element    Port    Amplitude       Phase
 phi   z                           (deg)
```

Fig. 4.21. The input file `cympa.in` *for calculation of radiation pattern of circularly polarized 1x4 element array*

The radiation patterns in the azimuthal and elevation planes are plotted in Figs. 4.22 - 4.25. In these figures, a comparison is given between results calculated using Cympa and measurements. The measurements were made by Dr. Michelle Champion at AFRL/SNHA , Hanscom AFB. Figure 4.26 showa comparison between calculated and measured return loss of the 4x1 array with the feeding structure included.

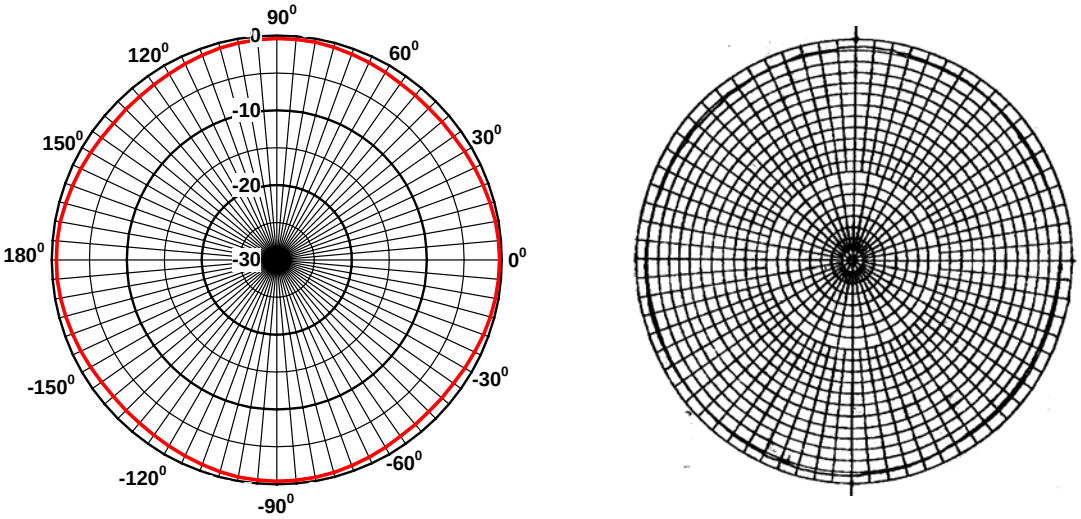

Fig. 4.22 - The comparison between calculated and measured radiation patterns of right-hand circular polarisation in azimuthal plane

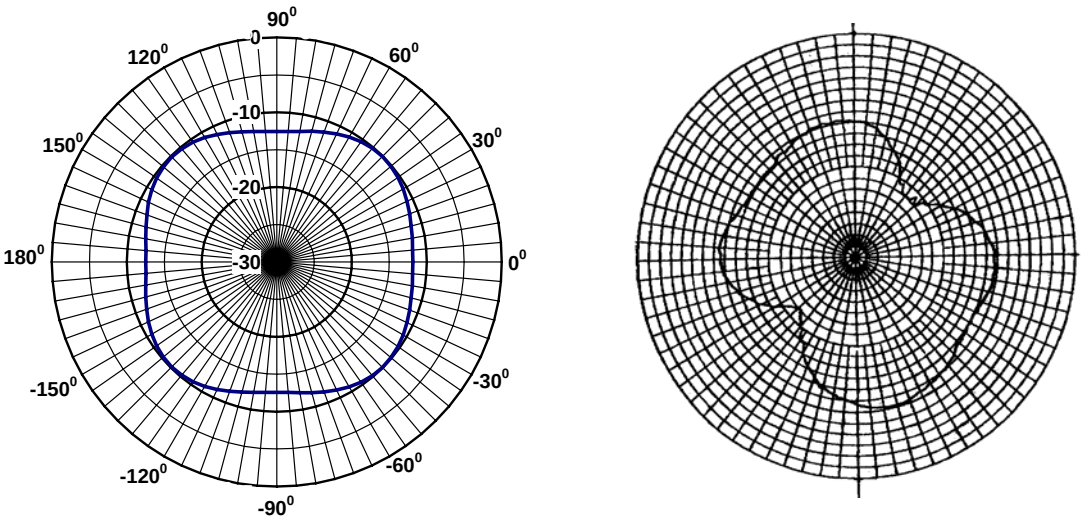

Fig. 4.23 - The comparison between calculated and measured radiation patterns of left-hand circular polarisation in azimuthal plane

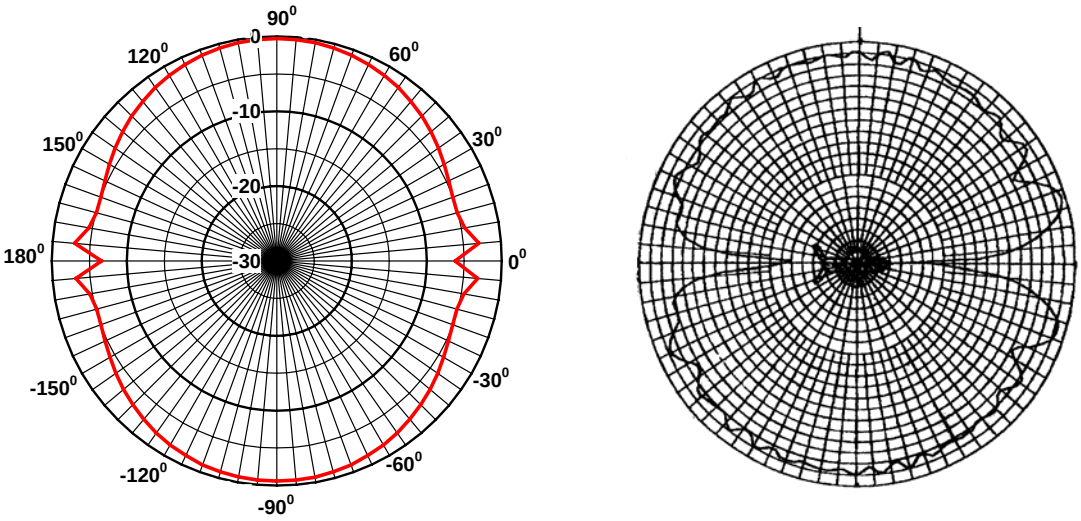

Fig. 4.24 - The comparison between calculated and measured radiation patterns of right-hand circular polarisation in elevation plane

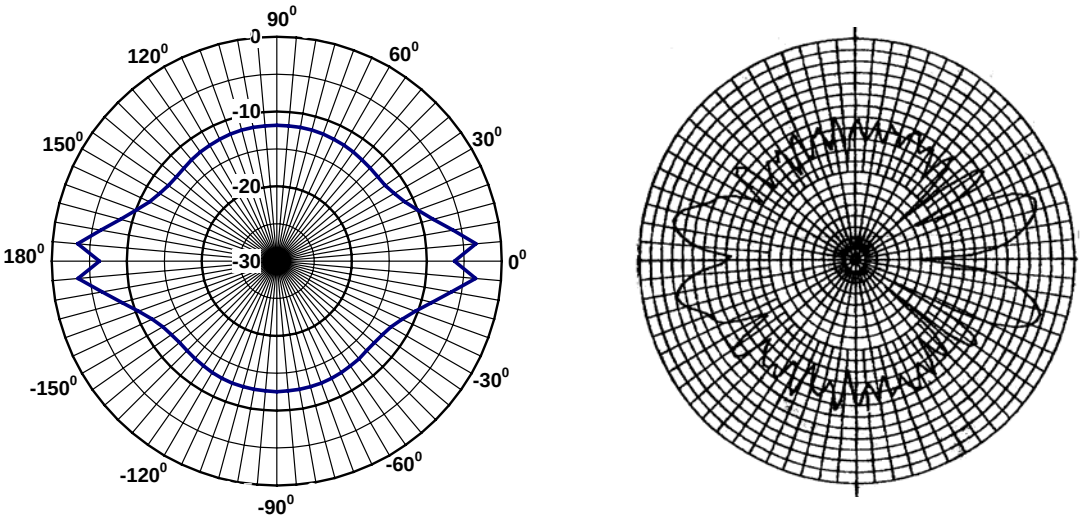

Fig. 4.25 - The comparison between calculated and measured radiation patterns of left-hand circular polarisation in elevation plane

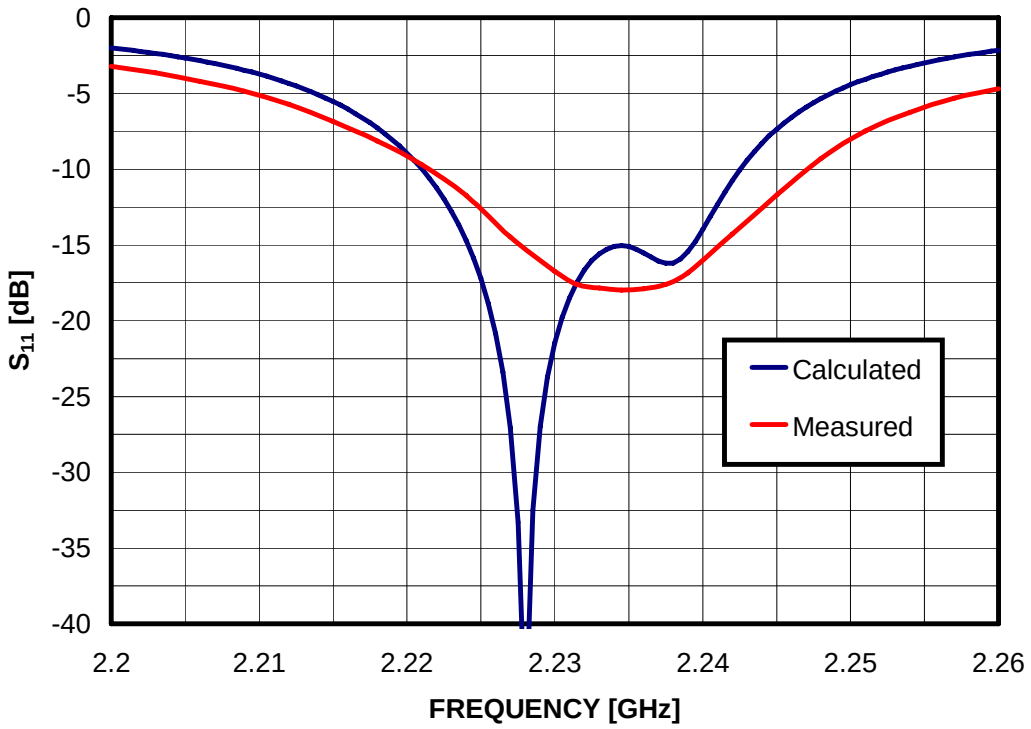

Fig. 4.26 - Calculated and measured return loss of the 4x1 array, with included feeding structure

4.3.4 RECTANGULAR PATCH FED BY MICROSTRIP LINE

This example shows the ability of rigorous calculation of microstrip fed square patch antenna of 5 cm x 5 cm dimensions. Two cases are analyzed, one with the cylinder of F_{GNG}=10 cm and one with the cylinder of F_{GNG}=2.5 cm. The content of input file as well as all the geometry data will be given for the first case, whereas for the second case the value of 10 cm for the radius is substituted with 2.5 cm.

ITEM	PARAMETERS	DESCRIPTION
frequency	1.95-2.05 GHz	frequency band in which the simulation is performed
radius of the grounded tube	ρ_{GND} = 10 cm	radius of the grounded tube
parameters of dielectric slab	h = 0.762 mm ε_r = 2.2 tan δ = 0.001	thickness relative permittivity
patch dimensions	w_ϕ = 5 cm w_Z = 5 cm	width of the patch in ϕ direction width of the patch in z direction
microstrip line feed position, related to patch center	ϕ_{FEED} = 0.0 cm z_{FEED} = 2.5 cm Z_0 = 50 Ω	in ϕ direction in z direction characteristic impedance

Table 4.6 - Properties of patches printed on cylindrical substrate in z direction (E plane)

The input file `cympa.in` is shown in fig. 4.27. Figure 4.28 and 4.29 show the results obtained with CyMPA and the comparison of these results with the measurements. The measurements are taken from [18]. It is interestng to observe how the input impedance decreases with the decrease of the tube radius.

```
 1.95      2.05      101          ! Frequency (GHz)
 10                               ! Ground tube radius (cm)
 1                                ! Number of dielectric layers
 0.0762    2.2       0.001        ! h, epsilon_r, tanges (delta)
 1                                ! Die. layer at which patches are placed
 1         1                      ! Number of patches in phi/z direction
 5.0       5.0                    ! Patch width in phi and z direction (cm)
 M                                ! Feed type (M - microstrip, C - coax)
 1                                ! Number of ports per patch
 0.0       2.5                    ! Feed position in phi and z direction (cm)
 Y                                ! Equal port excitation (Y - yes, N - no)
12.0       12.5                    ! Distance between patch centers
50.0       0.229                   ! Characteristic impedance of the feed line
180                               ! Number of phi modes in Fourier series
-180.0       180.0     361         ! Azimuthal pattern
 1.0         179.0     179         ! Elevation pattern
 0.0                               ! Phi angle of the evelation pattern
90.0      0.0                     ! Theta and phi angle of the main beam
 L                                ! Polarization (L - linear, C - circular)
 1                ! Mode of calculating the radiation pattern
                  !  1 = rigorous method
                  !  2 = simple model, uniform excitation
                  !  3 = simple model, file for patch excitations
                  !  4 = simple model, maximum predefined, corrected phases
```

Fig. 4.27. The input file `cympa.in` *for calculation of input impedance of a patch fed by microstrip line*

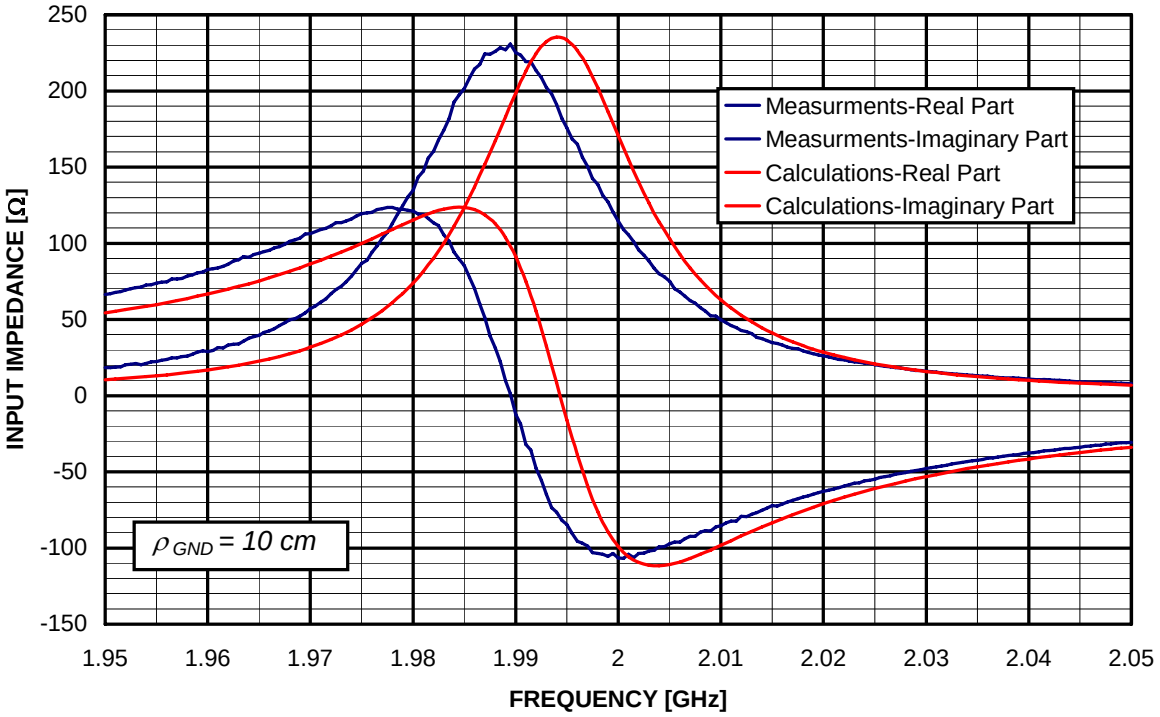

Fig. 4.28 - The input impedance of the single patch printed on the cylindrical substrate of 10 cm radius and fed by microstrip line. A comparison of calculations performed by CyMPA and measurements.

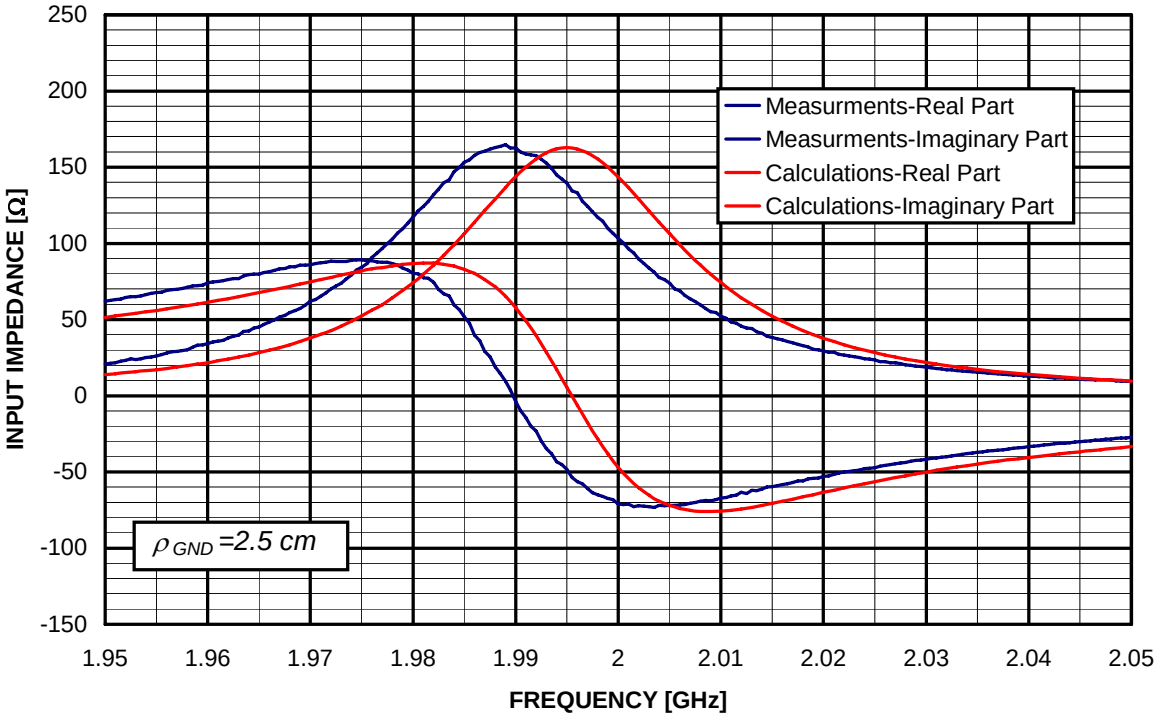

Fig. 4.29 - The input impedance of the single patch printed on the cylindrical substrate of 2.5 cm radius and fed by microstrip line. A comparison of calculations performed by CyMPA and measurements.

5 CONCLUSIONS AND PERSPECTIVES

We have developed a program for analyzing microstrip patch arrays printed on circular cylindrical structures. It is assumed that the patches are rectangular and that they are placed periodically in axial and circumferential direction. Two types of feeding structure are considered: microstrip transmission line and coaxial transmission line. The program solves the electric field integral equation, and the moment method is used for solving the integral equation. The possibility of analyzing patch antennas printed on multilayer structures is obtained by implementing a routine for calculating Green's functions of multilayer cylindrical structures. The numerical evaluation of elements used in moment method is made with special care. In particular, numerical treatment of Bessel and Hankel functions, and selection of the contour of integration were carefully made in order to ensure reliable and fast evaluation of the elements needed for the moment method procedure.

The program calculates the following parameters of the cylindrical patch arrays:

- input impedance at each input port in the array
- mutual coupling between each two patches in the array
- radiation pattern of the array.

In order to make first design of the array fast and easy, a possibility of calculating the radiation pattern in a simple way is implemented. In this mode mutual coupling between patch elements is not taken into account. This mode of the radiation pattern calculation is suitable for connection with some optimization procedure in order to achieve desirable radiation characteristics.

The program is tested by comparing the calculated results and measurements. The measurements were provided by AFRL/SNHA, Hanscom AFB, and some of them were found in literature. In all tested cases there is a good agreement between measurements and calculated results.

The perspective of continuation of the project follows two directions:

1. **Modeling of the aperture coupled cylindrical patch antennas**. This type of program is useful in constructing conformal active phased array. Conventional active phased arrays consist of radiating elements, T/R modules and a beamforming network. They are not widely used in practice since they are thick, heavy, expensive, and they require large amounts of power. The new technology of Micro Electro Mechanical Switches (MEMS) will enable the production of low-loss phase shifters, and therefore disadvantages of active phased arrays will be reduced. The newly proposed designs consist of several boards sandwiched together, and the connection between the stripline matching network and the radiating patches will be via apertures in the ground plane. Therefore, there is a need for the software that can analyze aperture coupled cylindrical patch antennas.

2. **Creation of a program for the radiation pattern synthesis**. The curvature effects significantly change the radiation pattern (in comparison to the planar case). Projective synthesis, where the known planar aperture distribution is projected to the conformal surface, gives poor results. Therefore, there is a need for more advanced methods. One idea is to connect the routine that calculates the radiation patter and some optimization routine like iterative least squares, genetic algorithm or simulated annealing. Furthermore, there is a need for analysis tools of non-equally spaced patch arrays. For example, by using slightly non-periodic arrays it is possible to suppress the grating lobes.

6 BIBLIOGRAPHY

[1] T. M. Habashy, S. M. Ali, and J. A. Kong, "Input impedance and radiation pattern of cylindrical-rectangular and wraparound microstrip antennas," *IEEE Trans. Antennas and Propagat.*, Vol. 38, pp. 722-731, May 1990.

[2] E.H. Newman, and J.H. Tehan, "Analysis of microstrip array and feed network," *IEEE Trans. Antennas and Propagat.*, Vol. 33, pp. 397-403, Apr. 1985.

[3] Z. Sipus, J. Bartolic, and B. Stipetic, "An approach to microstrip patch elements and array design", *Proceedings of COST 223-ESA Workshop on Active Antennas*, ESA-ESTEC, Noordwijk, The Netherlands, 1992, pp. 3.5.1-3.5.8.

[4] Z. Sipus, J. Bartolic, and B. Stipetic, "Input impedance of rectangular patch antenna fed by microstrip line, *Electronics Letters*, Vol. 28, No. 20, pp. 1886-1888, Sep. 1992. Errata, *Electronics Letters*, Vol. 28, No. 23, pp. 2199, Nov. 1992.

[5] Z. Sipus, P.-S. Kildal, R. Leijon, and M. Johansson, "An algorithm for calculating Green's functions for planar, circular cylindrical and spherical multilayer substrates," *Applied Computational Electromagnetics Society Journal,* Vol. 13, No. 3., pp. 243-254, Nov. 1998.

[6] L.B. Felsen, and N. Marcuvitz, *Radiation and Scattering of waves*, Englewood Cliffs, NJ: Prentice Hall, 1973, ch. 6.

[7] W. C. Chew, *Waves and fields in inhomogeneous media*, IEEE Press, New York, 1995.

[8] U.V. Gothelf, and A. Ostergaard, "Full-wave analysis of a two slot microstrip filter using a new algorithm for computation of spectral integrals," *IEEE Trans. Microwave Theory Tech.*, Vol. 41, pp. 101-107, Jan. 1993.

[9] D.M. Pozar, and S. M. Voda, "A rigorous analysis of a microstrip line fed patch antenna", *IEEE Trans. Antennas and Propagat.*, Vol. 35, pp. 1343-1349, Dec. 1987.

[10] G. Vecchi, T. Bertuch, and M. Orefice, "Analysis of cylindrical printed antennas with subsectional basis functions in spectral domain," *Proc. ICEAA 1997.*, Torino, Italy, Sep. 1997, pp.301-304.

[11] R.F. Harrington, *Time-harmonic electromagnetic fields*, McGraw-Hill, New York, 1961, p. 245.

[12] D.M. Pozar, "Input impedance and mutual coupling of rectangular microstrip antennas", *IEEE Trans. Antennas and Propagat.*, Vol. 30, pp. 1191-1196, Nov. 1982.

[13] J. B. Knorr, 'Consequences of symmetry in the computation of characteristic modes for conducting bodies', *IEEE Trans. Antennas and Propagat.*, vol. 21, Nov 1973, pp. 899-902.

[14] M. Hamermesh, *Group theory and its application to physical problems*, Pergamon Press, New York, 1964, pp. 111-113.

[15] M. Tinkham, *Group theory and quantum mechanics*, McGraw-Hill, New York, 1964, p. 80.

[16] K.L. Wong, and G.B. Hsieh, "Curvature effects on the radiation patterns of cylindrical microstrip arrays", *Microwave and Optical Technology Letters*, Vol. 18, No. 3, pp. 206-209, June 1998.

[17] W.Y. Tam, A.K.Y. Lai, and K.M. Luk, "Mutual coupling between cylindrical rectangular microstrip antennas," *IEEE Trans. Antennas and Propagat.*, Vol. 43, pp. 897-899, Aug. 1990.

[18] R. Staraj, G, Ghio, J.-P. Damiano, "Experimental study of curvature and line width effects on characteristics of printed antennas fed by microstrip line," *Proc. JINA 1996.*, Nice, France, Nov. 1996, pp.368-371.